UNIVERSITÀ
DEGLI STUDI
DI PADOVA

Sede Amministrativa: Università degli Studi di Padova

Dipartimento di Scienze Biomediche Sperimentali

SCUOLA DI DOTTORATO DI RICERCA IN: BIOSCIENZE
INDIRIZZO: BIOLOGIA CELLULARE
CICLO: XXII

STRUCTURAL AND FUNCTIONAL STUDIES OF SNAKE PHOSPHOLIPASE A_2 NEUROTOXINS

Direttore della Scuola: Ch.mo Prof. Tullio Pozzan
Coordinatore d'indirizzo: Ch.mo Prof. Cesare Montecucco
Supervisore: Ch.mo Prof. Cesare Montecucco

Dottorando : Marco Paoli

A Giò

Mi chiedo perché il dubbio
appare agli uomini come una felicità.

da *Vita di Galileo* di *Bertold Brecht*

INDEX

SUMMARY

Snake presynaptic neurotoxins with phospholipase A_2 activity are potent inducers of paralysis through the inhibition of the neuromuscular junction. These neurotoxins were recently shown to induce exocytosis of synaptic vesicles following the production of lysophospholipids and fatty acids and a sustained influx of Ca^{2+} from the external medium. Here, we have performed some functional studies on their mechanism of intoxication, showing that snake PLA_2 neurotoxins are able to penetrate neuronal cells after five minutes of intoxication. We reported that internalized snake neurotoxins specifically localize on mitochondria. We show here that presynaptic phospholipase A_2 neurotoxins facilitate opening of the mitochondrial permeability transition pore, resulting in a negative effect on mitochondria calcium buffering capacity. Successively, it has been studied the effective phospholipase A_2 activity of the toxins during intoxication. The time-course of phospholipid hydrolysis in cerebellar neuronal cultures intoxicated with four different snake neurotoxins was monitored. Our findings partially explain the high discrepancy between lethal potency and *in vitro* measured activity reported in literature for the four considered neurotoxins. However, the most toxic textilotoxin and taipoxin still showed lower enzymatic activities on neurons than those of notexin and β-bungarotoxin, therefore, one must invoke more favorable pharmacokinetics to account for the remaining difference in toxicity. Furthermore, it was here identified the outer layer of the plasma membrane as the main target of phospholipase A_2 neurotoxins hydrolysis. Nevertheless, limited intracellular activity concentrated on specific targets must not be excluded. For a better comprehension of the high toxicity of multimeric snake PLA_2 neurotoxins with respect to the monomeric ones, studies on the quaternary structure of taipoxin are in progress. We present here the crystallographic structure of beta subunit, one of the three PLA_2 subunits of taipoxin, with preliminary considerations.

SOMMARIO

Le neurotossine con attività fosfolipasica di tipo A_2, isolate dal veleno di alcune famiglie di serpenti, inducono la paralisi della giunzione neuromuscolare. Tali tossine riconoscono in maniera altamente specifica il terminale presinaptico, idrolizzano i fosfolipidi di membrana del foglietto esterno inducendo una modifica strutturale della plasmamebrana, alterazione che facilita la fusione delle vescicole sinaptiche e ne inibisce l'endocitosi. In questo lavoro sono presentati i risultati ottenuti durante alcuni studi funzionali sul meccanismo d'azione delle neurotossine di serpente. Le evidenze sperimentali qui riportate, dimostrano che le neurotossine studiate sono in grado di superare la membrana cellulare e di localizzarsi a livello mitocondriale. Successivi studi *in vitro*, condotti su mitocondri isolati, rivelano come tali neurotossine siano in grado di indurre l'apertura del poro di permeabilità mitocondriale e, conseguentemente, di influire negativamente sulla abilità dei mitocondri di assorbire calcio dal mezzo circostante. In seguito è stata misurata l'attività enzimatica di quattro neurotossine di serpente con attività fosfolipasica di tipo A_2 su colture neuronali di granuli di cervelletto. L'attività idrolitica delle neurotossine è stata monitorata nel tempo, rivelando una maggiore omogeneità di attività fra le diverse tossine rispetto a quanto osservato in esperimenti condotti su substrati artificiali. Si riporta comunque una discrepanza fra tossicità e attività enzimatica delle neurotossine studiate, probabilmente dovuta ad una farmacocinetica favorevole alle neurotossine più complesse, le quali, pur presentando attività enzimatica minore, risultano maggiormente neurotossiche. Queste misure hanno inoltre permesso di individuare nel foglietto esterno della membrana plasmatica il target principale dell'attività idrolitica delle tossine in questione. Concludendo, si presentano alcuni studi preliminari alla caratterizzazione della struttura quaternaria della tossina trimerica taipoxin.

1

GENERAL INTRODUCTION

1.1 Clinical relevance

Envenoming resulting from snake bites is an important public health hazard in many regions, particularly in tropical and subtropical countries. Although antivenoms are being produced by several laboratories, precarious economic conditions and lack of facilities in the interested countries, make snake bite envenoming a major problem of great impact on third world nations health care systems. Unfortunately, public health authorities, nationally and internationally, have given little attention to this problem, relegating snake bite envenoming to the category of a major neglected disease (Theakson *et al.*, 2003).

Most severe cases of snake bite envenoming are inflicted by species of the family Elapidae (cobras, kraits, mambas, Australasian species, and sea snakes) and the family Viperidae (rattlesnakes, lance-headed pit vipers, and true vipers). The species causing the largest numbers of bites and fatalities are *Echis sp.* (saw-scaled vipers) in northern Africa, *Bothrops asper* and *B. atrox* (lance-headed pit vipers) in Central and South America, and *Naja sp.* (cobras) and *Bungarus sp.* (kraits) in Asia and Australia.

Envenoming of most elapid snakes induce some life-threatening systemic effects. Neuromuscular transmission blockade is a typical consequence of elapid snakes bites, attributable to effects of pre- and/or post-synaptically acting neurotoxins targeting neuromuscular junctions. These toxins cause progressive descending paralysis, which may become life-threatening when bulbar and respiratory muscles are involved. In envenomings by several elapid snakes and some viperids, such as South American rattlesnakes, there is a generalised rhabdomyolysis induced by phospholipases A_2 (PLA_2), which may cause myoglobinaemia, hyperkalaemia, and acute renal failure. Envenomings by elapids, such as African spitting cobras and some Asian cobras, also induce local necrosis. Such local pathology is mostly due to the action of phospholipases A_2 and zinc-dependent metalloproteinases. These local effects develop rapidly after the bite; consequently, a delay in the access to health facilities frequently results in drastic tissue damage and permanent disability.

The major protein components responsible for the elevated toxicity of elapid snakes are phospholipase A_2 homologous proteins extremely specific for the neuromuscular junction, whose major effect is the persistent blockade of neurotransmitter release in the peripheral nerve terminals. These proteins have evolved from an ancestral secretory PLA_2 with digestive function. They fold very similarly and display a range of enzymatic turnover values from zero to the high values typical of digestive enzymes such as those found in pancreatic secretions.

Since venoms serve in both immobilization and digestion of the pray, they have evolved to have a strong balance in their toxic and digestive components. In this frame, snake PLA_2 neurotoxins constitute a excellent example of combination of lethal toxicity and digestive properties not only in the same venomous mixture, but in the very same protein (Gutierrez *et al.*, 2006).

1.2 Structure and function of presynaptic PLA_2 neurotoxins

Snake presynaptic phospholipase A_2 neurotoxins (SPANs) are Ca^{2+}-dependent secretory phospholipase A_2 ($sPLA_2$) enzymes endowed with high neuronal specificity and involved in neurotransmission blockade. Phospholipase A_2 neurotoxins constitute a very heterogeneous protein group in terms of quaternary structure, with a common structural unit homologous to the common non-neurotoxic pancreatic secretory PLA_2. As far as the structural complexity is concerned, SPANs possess a certain variability, but only the crystallographic structures of some of the simpler toxins have been determined (Westerlund *et al.*, 1992; Kwong *et al.*, 1995; Singh *et al.*, 2001). The high resolution structures of monomeric PLA_2 neurotoxins show a very well conserved folding pattern and molecular weights ranging from 13 to 15 kDa. Fourteen conserved cysteins form a network of seven disulphide bridges which stabilize the protein tertiary structure. The structure includes three α-helices and a calcium-binding loop, which constitute the PLA_2 enzymatic core, plus two antiparallel β-sheets, poorly conserved in sequence, and probably endowed with anticoagulant properties. Amino acid side-chains arising from the enzymatic core coordinate the calcium ion essential for the hydrolysis reaction. Moreover, they define the hydrophobic pocket which accommodates the phospholipidic substrate and mediate the events of catalysis (Kini, 1997). All monomeric $sPLA_2$s share a high structural similarity and only few aminoacid changes are enough to convert a non-toxic pancreatic $sPLA_2$ into the highly toxic snake PLA_2s suggesting that the neurospecificity is due to minor alterations of the exposed residues, rather than to major structural changes. The monomeric one is the most common and simplest form in which SPANs can be found, but not the only one. In fact, PLA_2 neurotoxins show a wide range of structural complexity. They can exist as monomers, such as notexin or ammodytoxin, whose structural details have already been well investigated (Westerlund *et al.*, 1992; Saul *et al.*, 2009), but they can also be bound via disulfide to an auxiliary structure as for β-bungarotoxin (Kwong *et al.*, 1995) or crotoxin (Hendon and Fraenkel-Conrat,

1971) or aggregate to form PLA_2-dimers as in *Vipera amodytoxin meridionalis* (Georgieva *et al.*, 2004). Greater complexity is achieved when $sPLA_2$s aggregates to form heterotrimers such as taipoxin (*Oxyuranus scutellatus scutellatus*; Fohlman *et al.*, 1976), paradoxin (*O. microlepidotus*; Fohlman *et al.*, 1979), or cannitoxin (*O. s. canni*; Kuruppu *et al.*, 2005), or heteropentamers (or hexamers) as in the case of textilotoxin (*Pseudonaja textilis textilis*; Tyler *et al.*, 1987; Aquilina, 2009). Up to date, no structural information is available on the quaternary structure of SPANs of complexity level above the dimeric aggregation state.

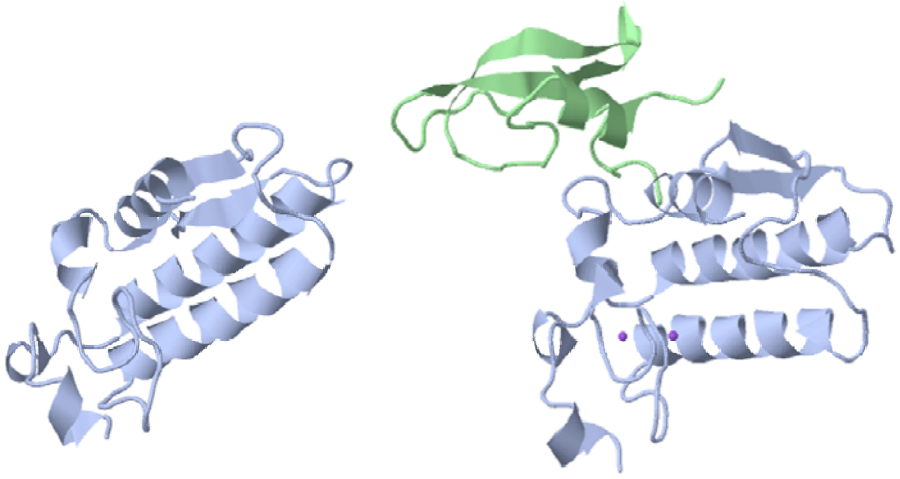

Figure 1. Three-dimensionl structures of notexin (left, Westerlund *et al.*, 1992) and β-bungarotoxin (right, Kwong *et al.*, 1995). In grey is colored the common PLA2 subunit, in green the dendrotoxin-like subunit of β-bungarotoxin .

Not only in structure but also in enzymatic activity and neurotoxicity, SPANs present a wide heterogeneity. The major effect of SPANs intoxication is the rapid paralysis of the neuromuscular junction due to the neurotransmission blockade. The neurotoxicity of PLA_2 can be measured either as time of paralysis of a nerve-muscle preparation or as mouse LD_{50} (the dose at which 50% of a mouse population dies upon intoxication). By means of nerve-muscle preparations, it is possible to monitor the reaction of the muscle upon nerve stimulation in intoxicated versus non-intoxicated samples. Following snake PLA_2 neurotoxin intoxication, it is generally reported a transient effect of facilitated neurotransmitter release, followed by a gradual and irreversible blockade of neurotransmission with consequent muscular paralysis (Kini, 1997; Rigoni *et al.*, 2004). However, the set of data available with this method is not as complete and homogeneous as the one obtained with the lethal dose 50% assay. The toxicity of snake PLA_2 neurotoxins, measured as mouse lethal dose 50% (mouse LD_{50}), ranges from being non-lethal at high amounts (25 mg/kg) to being among the

most lethal animal products (textilotoxin mouseLD_{50} = 0,001 mg/kg, see Table 1). The catalytic activity is also extremely variable. As reported in Table 1 (data from Kini, 1997), the amount of nmols of phospholipids hydrolyzed per minute from one nmol of PLA_2 neurotoxin may vary more than a thousand fold for different SPANs. No direct relationship has been found between the relative enzymatic activities of snake PLA_2 neurotoxins and their lethal potencies. Nevertheless, neurotoxicity results from the coexistence in the toxins of two factors: (1) the capacity of hydrolyzing efficiently the phospholipids of the presynaptic membrane, and (2) the ability to recognize the nerve terminal, to bind efficiently to it, and to concentrate in that site the enzymatic activity.

1.3 Previous studies

The first studies on the mechanisms of action of presynaptic PLA_2 toxins were conducted by Chang and Lee (1963). Using neuromuscular preparations, they determined that β-bungarotoxin blocked the nerve mediated twitch of the rat phrenic nerve-diaphragm preparation. Only a brief period of exposure to the toxin is required to subsequently block the twitch, suggesting that the binding is not the limiting step and that once binding occurs the block is irreversible. A latency to onset of neuromuscular blockade was observed, but it could be reduced by increasing toxin concentration or stimulation frequency. *Via* the nerve-muscle study model, and in presence of low calcium to increase the sensitivity of the preparation, it was possible to identify three phases in SPANs intoxication: the initial phase consists of a rapid decline in twitch height; this is followed shortly after by an increase in neurotransmitter release and therefore in twitch height; third and last phase is a gradual and complete decrease of the transmission until complete blockade occurs. Furthermore, the finding that increased nerve stimulation frequency can shorten the paralysis time suggested that the molecular basis of the SPANs-induced neurotransmission blockade was linked to synaptic vesicle (SV) turnover (Chang *et al.*, 1973).

Some hints on the internalization of SPANs were given by neutralization experiments conducted on synaptosomes. It was observed that β-bungarotoxin becomes inaccessible to neutralizing antibodies after about 15 minutes of intoxication in nerve-muscle preparations. Moreover, the action of presynaptically active PLA_2 toxins was not antagonized by drugs impairing the internalization of botulinum neurotoxin, suggesting a different way of internalization than the SV recycling pathway (Simpson *et al.*, 1993).

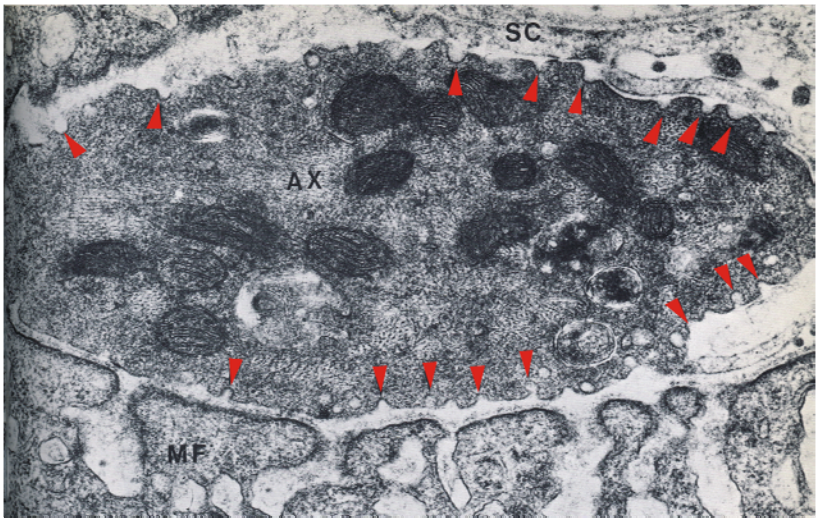

Figure 2. Electron microscopy analysis of neuromuscular junction of phrenic nerve-hemidiaphragm preparation intoxicated with taipoxin (46,000x). The axon terminal is almost devoid of synaptic vesicles and shows numerous axolemmal indentations (red arrowheads). Adapted from Cull-Candy *et al.*, 1976.

Ultrastructural observation of intoxicated periferic nerve terminals provided some basis for an interpretation of the physiological findings abovementioned. Taipoxin treatment was reported to cause an enlargement of the terminal with major depletion of both ready-to-release and reserve pool synaptic vesicles in the intoxicated nerve terminals. The SV depletion correlates with the level of envenomation of the nerve, thereby offering a morphological correlation to the gradual reduction of the neurotransmitter release. several clathrin-coated indentations are visible All along the presynaptic plasma membrane of the intoxicated neuromuscular junction are visible recurrent clathrin-coated indentations,, suggesting an abnormal persistence of an exo/endocytotic process. Moreover, in the analized nerve muscular junction, mitochondria appear swollen with altered cristae, in agreement with alteration of mitochondrial membrane potential observed in intoxicated synaptosomes (Cull-Candy et al., 1976; Kini, 1997) and with what more recently observed in primary neuronal cells (Rigoni et al., 2007).

1.4 Recent achievements and findings here reported

More recently, some major steps towards the comprehension of snake PLA_2 intoxication mechanism were obtained in our research group. The major goals have been the demonstration that (1) the enlargement of the terminals and the

bulging of accessible neuronal processes is due to massive increase of membrane due to the enhanced SV fusion, (2) that the enzymatic activity is an essential component of SPANs neurotoxicity, even if not sufficient and even if not correlated with neurotoxicity, and (3) that upon intoxication it takes place an impairment of mitochondria functionality and a pronounced increase of intracellular Ca^{2+} concentration due to calcium ions leak through the altered plasma membrane.

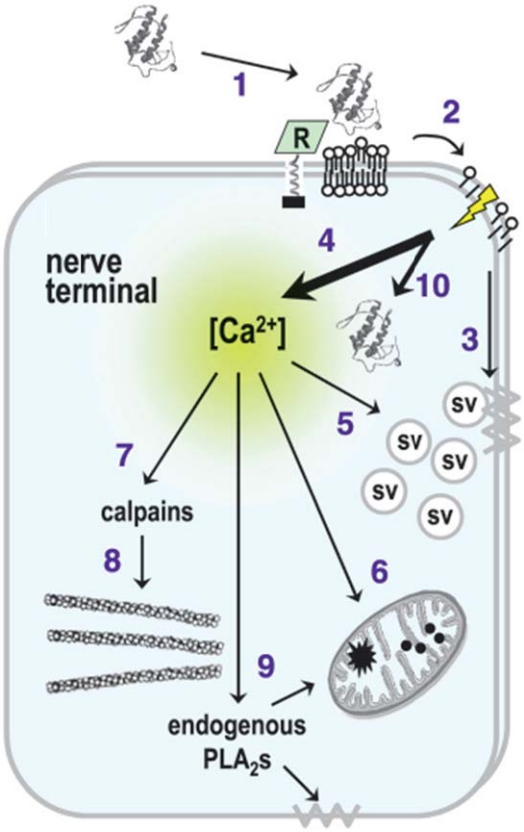

Figure 3. Schematic representation of the action of a neurotoxic snake PLA_2 on motor nerve terminals. Step 1 represents the neurotoxins binding either to high-affinity specific protein receptors (R) or to low-affinity lipid domains of the plasmamembrane. Step 2 is the hydrolysis of phospholipids that takes place after binding, followed by alteration of the membrane structure. Disrupted plasmamembrane becomes permeable to ions, thus losing its membrane potential and allowing a large influx of Ca^{2+} from the extracellular medium. Such altered membrane promotes the exocytosis of ready-to-release synaptic vesicles at the nerve terminal (step 3). Moreover, the large increment of cytosolic Ca^{2+} causes the exocytosis of the synaptic vesicle reserve pool (step 5). Ca^{2+} uptake by mitochondria, through the uniporter, results in mitochondrial swelling, disorganization of cristae, formation of hydroxyapatite crystals and flocculent densities, resulting in a severe impairment of mitochondrial function (step 6). Ca^{2+}-dependent proteinases (calpains) are activated and degrade cytoskeletal components (step 7 and 8), further affecting the mechanical integration of the cell. Ca^{2+}-dependent cytosolic PLA_2s are activated and promote further hydrolysis of intracellular membranes and plasma membrane (step 9). Plasma membrane disruption allows the entry of neurotoxins (step 10), which hydrolyze and damage intracellular membrane systems, until inactivated by yet undetermined molecular events. Adapted from Montecucco *et al.*, 2008.

A first important achievement was the observation that upon neuron intoxication there is an increase in plasma membrane in discrete regions, identified morphologically by rounded bulges along the neuronal processes. Interestingly, these findings closely match the conclusions drawn after electron microscopy observations of intoxicated neuromuscular junctions, which appear swollen, depleted of SVs and enriched in clathrin-coated invaginations of the plasma membrane representing incomplete SV retrieval (Chen and Lee, 1970; Cull-Candy *et al.*, 1976). To investigate the nature of the bulges possibly due to the massive induction of SV exocytosis, immunostaining experiments were performed. Hence, it was observed that the enlargements were enriched in SV membrane proteins and that markers of the vesicular lumen become exposed on the neuronal surface in correspondence of the enlargements (Rigoni *et al.*,2004), demonstrating that the observed phenotype results from the fusion of synaptic vesicles with the plasma membrane not balanced by an adequate membrane retrieval.

A further step towards the understanding of SPANs mechanism of action, has been the demonstration that the hydrolytic activity is a necessary factor of snake PLA_2 neurotoxicity. The role of the phospholipase A_2 activity in the mechanism of intoxication has always been ambiguous. Indeed, there is only a partial correlation between PLA_2 activity and neurotoxicity among SPANs and there is no overlap of surface residues required for neurotoxicity with those essential for PLA_2 activity. In 2005, Rigoni and colleagues compared on mouse nerve phrenic-hemidiaphragm preparation and on primary neuronal cultures, the effects of SPANs with those of their hydrolysis products: lysophospholipids (LysoPLs) and fatty acids (FAs). The striking finding was that all the effects observed in intoxicated models could be detected also when the lysophospholipids and fatty acids aequimolar mixture was employed instead of the SPANs (Rigoni *et al.*, 2005; Caccin *et al.*, 2006; Caccin *et al.*, 2009). Those experiments clarified that the phospholipase activity is not a mere conserved property of snake PLA_2 neurotoxins, but it is determinant for their toxic effect.

The massive induction of SV fusion and the requirement of the PLA_2 activity for the intoxication of presynaptic nerve terminals cleared the way to the comprehension of the molecular mechanism of SPANs primary toxic effect. The property of PLA_2 neurotoxins to concentrate their catalytic action at specific sites of the presynaptic membrane, generates a significant local amount of phospholipids hydrolysis. The produced fatty acids equally distribute among the lipid bilayer with no immediate consequences for the plasma membrane. Instead, lysophospholipids are forced to remain on the outer leaflet due to the high energy required for their hydrophilic head to cross the membrane. The presence of lysophospholipids and fatty acids within the plasma membrane has three major consequences: (1) the accumulation of significant amounts of lysospecies

on the outer layer of the plasma membrane confers to the lipid bilayer a positive curvature which promotes ready-to-release vesicle fusion and inhibits a proportionate synaptic vesicle retrieval (Rigoni *et al.*, 2005; Rossetto and Montecucco, 2008); (2) phospholipids degradation increases the membrane permeability to calcium (Rigoni *et al.*, 2007), whose significant increase is well known to trigger the exocytosis of all the vesicles present in the nerve terminal (Ceccarelli *et al.*, 1972; Rizzoli and Betz, 2005); (3), contrarily to lysophospholipids, fatty acids are allowed to diffuse freely to different layers of the membrane and may eventually partition into intracellular organelles and alter their function. In particular, *in vivo* studies of mitochondria in intoxicated neurons showed a progressive loss of membrane potential with parallel changes in morphology from an elongated to an inactive rounded shape (Rigoni *et al.*, 2007). Different factors could potentially contribute to this mitochondrial impairment: (1) fatty acids, as mentioned above, are known to partition into intracellular membranes and may act as mitochondrial uncouplers, and (2) an accumulation of Ca^{2+} inside the mitochondrial matrix, due to the increase in intracellular Ca^{2+} concentration upon SPANs intoxication. Therefore, mitochondrial damage appeared to have a major role in the mechanism of SPANs poisoning of nerve terminals and this findings were in agreement with previous *in vitro* studies performed with β-bungarotoxin on synaptosomes (Ng and Howard, 1978; Rugolo *et al.*, 1986).

It also needs to be considered that not only fatty acids can diffuse into intracellular membranes, but also SPANs themselves may enter and bind to the internal membranes hydrolyzing phospholipids in loco. In fact, it was observed that intoxication can be neutralized by anti-toxin antibodies or by washing only at early intoxication time. At prolonged intoxication time, the neurotoxins seem to disappear from the outside of the neuronal cell and the toxin effect cannot be any longer neutralized, suggesting an internalization of the toxins inside the nerve terminal (Kamenskaya and Thesleff,1974; Simpson *et al.*, 1993). Successive studies further supported the hypothesis that SPANs can gain access to the cell interior. Indeed, fluorescein-conjugated β-bungarotoxin was found to rapidly enter hippocampal neurons and it was suggested to associate at least in part with lysosomes (Herkert *et al.*, 2001). Taipoxin was found to localize inside chromaffin cells in culture (Neco *et al.*, 2003), and to interact *in vitro* with an endoplasmic reticulum-located protein (Dodds *et al.*, 1995). Furthermore, ammodytoxin A (a PLA_2 neurotoxin isolated from the venom of *Vipera ammodytes*) was detected in the nucleus of hippocampal neurons (Petrovic *et al.*, 2004) and it was found to interact with cytosolic and mitochondrial proteins (Sribar *et al.*, 2001; 2003a; 2003b). Little is known on the mechanism of internalization of snake PLA_2 neurotoxins, nor on the role of the catalytic activity in the entry process.

However, the inability to enter the neurons observed in Sr^{2+} inactivated neurotoxins (Praznikar *et al.*, 2008) suggests that SPANs may require phospholipid hydrolysis to alter the membrane in such a way as to promote their own translocation into the cytosol.

Our recent findings here shown, confirm that snake PLA_2 neurotoxins, conjugated to fluorescent dyes, are indeed able to penetrate spinal cord motor neurons and cerebellar granule neurons. Furthermore, after their entrance they selectively bind to mitochondria. As a result of this interaction, mitochondria depolarize and undergo a profound shape change from elongated to round and swollen. Moreover, we report that the interaction between SPANs and mitochondria results in the enhancement of the opening of the mitochondrial permeability transition pore, an inner membrane high-conductance channel. The relative potency of the snake neurotoxins for the permeability transition pore opening correlates with their hydrolytic activity rather than with their neurotoxicity, suggesting a causal relationship between phospholipid hydrolysis and mitochondrial pore opening facilitation. This consideration is also supported by the effect of phospholipid hydrolysis products, lysophospholipids and fatty acids, on mitochondrial pore opening. These findings contribute to define the cellular events that lead to intoxication of nerve terminals by these snake neurotoxins and suggest that mitochondrial impairment is an important determinant of their toxicity.

Another aspect here investigated, is the contribution of the phospholipase A_2 activity to the toxic effect *in vivo*. The hydrolytic activity time course of four neurotoxins with different lethal potency and PLA_2 activity was monitored on a substrate of cerebellar granule neurons. On the opposite of classical PLA_2 activity assays, performed on artificial substrates, the analysis of snake neurotoxins hydrolytic activity on a cellular substrate provides information on their physiological hydrolytic effect (which is dependent on parameters such as binding and plasma membrane organization which are not considered in an *in vitro* assay). Our findings partially explain the high discrepancy between lethal potency and *in vitro* measured activity reported in literature for the four considered neurotoxins. However, the most toxic textilotoxin and taipoxin still showed lower enzymatic activities on neurons than those of notexin and β-bungarotoxin, therefore, one must invoke more favorable pharmacokinetics to account for the remaining difference in toxicity. The second important finding of this analysis has been the indication that the major site of phospholipid hydrolysis is the external site of the presynaptic membrane. In fact, our studies show a minimal hydrolysis of phospholipids characteristic of the the cytosolic side of the membrane (notably, phosphatidylethanolammine and phosphatidylserine) with respect to the hydrolysis measured for

phosphatidylcholine, more present on the exernal surface. Internal activity is however not excluded. In fact, limited hydrolysis concentrated on specific targets may generate a high local concentration of hydrolytic products and become thereafter of great relevance (as it will be discussed in chapter 2).

In the end, some preliminary data on the crystal structure of a single subunit of the trimeric toxin taipoxin are discussed. The structures of monomeric and dimeric neurotoxins have been extensively described, but there is a lack of structural information on toxins of more complex aggregation level. Indeed, a greater knowledge of multimeric neurotoxin quaternary structure could help us to understand the basis of the high specificity for the presynaptic nerve terminal reported for taipoxin or textilotoxin, and the consequent high lethal potency of multimeric toxins (Rossetto and Montecucco, 2008).

Figure 4. *Notechis scutatus* (top left), *Bungarus multicinctus* (top right), *Oxyuranus scutellatus* (bottom left), and *Pseudonaja textilis* (bottom right) are elapid snakes originary from Australia and South East of Asia. They venom contains the highly neurotoxic phospholipase A2 responsible for the neuromuscular paralysis of their prey.

Four snake PLA_2 neurotoxins have been considered in my studies: notexin, β-bungarotoxin, taipoxin, and textilotoxin. They show different structural complexity, but they are all composed by one or more homologous PLA_2 subunits. All four are extremely neurotoxic but very heterogeneous both in toxicity and in enzymatic activity:

Notexin (Ntx) is a single chain secretory PLA_2 of 119 amino acids cross-linked by seven disulfide bridges purified from the venom of the Australian tiger

snake (*Notechis scutatus scutatus*; Halpert and Eaker, 1975). It possesses a 55% amino acid sequence homology with the non neurotoxic porcine pancreatic $sPLA_2$ (included 12 of the 14 cysteines that stabilize the tertiary structure by mean of S-S bridges). Crystallographic structure is available, and high structural homology with other monomeric $sPLA_2$ is shown (Westerlund *et al.*, 1992);

β-bungarotoxin (β-Btx), purified from the venom of the multi-banded krait, *Bungarus multicinctus*, is an heterodimeric SPAN composed by an active PLA_2 subunit of 13,5 kDa linked via a disulphide bridge to a dendrotoxin-like 7 kDa unit (Kondo *et al.*, 1978). The dendrotoxin-like subunit (also homologous to a trypsin inhibitor) interacts with the presynaptic potassium channels, thus improving significantly the neuronal specificity of the toxin and hence its neurotoxicity (Rugolo *et al.*, 1986).

Taipoxin, purified from the venom of the Australian taipan snake (*Oxyuranus s. cutellatus*), is a 1 : 1 : 1 ternary complex of homologous PLA_2 subunits named alpha, beta, and gamma. The alpha and beta components consist respectively of 119 and 118 amino acid residues cross-linked by seven intramolecular disulfide bridges, whereas the gamma component has 133 residues and eight disulfides. Two iso-components of the beta subunit, beta-1 and beta-2, with a slight difference in amino acid composition, have been described (Fohlman *et al.*, 1976). Functional analysis on single subunits revealed that the alpha subunit is the only which fully conserves the phospholipase A_2 activity. Moreover, it was observed that the activity of alpha subunit alone is greater than the trimeric complex activity (Fohlman *et al.*, 1979). No data on the quaternary structure have been published yet.

Textilotoxin (purified from the venom of the Australian eastern brown snake, *Pseudonaja t. textilis*) is a multichain complex of five or six homologous PLA_2 units (there is still an open debate on textilotoxin aggregation state; Tyler *et al.*, 1987; Aquilina, 2009). Its subunits are hold together by non covalent interactions, with the exception of two subunits (D_2), which are linked by a disulphide bridge (Pearson *et al.*, 1991). Only one of the four isolated subunits (named from A to D) fully conserves the enzymatic activity, and such activity, as for taipoxin, is greater than the activity observed for the multimeric complex (Tyler et al., 1987). Recently, it was also reported how the subunit composition appears to be non homogeneous in the multichain complexes, increasing the complexity of a proper characterization of the toxin (Aquilina, 2009). Together with taipoxin, it shows a very low mouse LD_{50}, and is reported to be among the most dangerous animal toxins.

The SPANs here considered are commonly found as major neurotoxic components of Elapidae snake venoms, but other families (i.e. Viperidae, Hydrophidae or Crotalidae) also show abundant presence of PLA_2 neurotoxins. The four studied neurotoxins possess common features such as the basic structural unit and the involvement on neurotransmission blockade, but differ in structural complexity, in neurotoxic potency and in phospholipase activity. The use of four different representatives of a class of neurotoxins has been necessary to allow us to extend our findings to the entire group of snake PLA_2 presynaptic neurotoxins.

Table 1 Comparison of subunit composition, molecular weight, toxicity and enzymatic activity of the four investigated snake PLA_2 neurotoxins.

sPLA2	**Subunits**	**MW (kDa)**	**mouse LD_{50} * (μg/kg)**	**PLA_2 activity *,†**
Notexin	1	14	17	19.460
β-Bungarotoxin	2	21	14	1281
Taipoxin	3	42	2	18
Textilotoxin	5 (6)	70 (84)	1	224

*from Kini, 1997. Lethal Potency of Snake Venom Phospholipase A_2 Enzymes

† in nmols of PL hydrolysed / min / nmol of toxin

References

Aquilina JA (2009) The major toxin from the Australian Common Brown Snake is a hexamer with unusual gas-phase dissociation properties. *Proteins* 75(2):478-85

Caccin P, Rigoni M, Bisceglie A, Rossetto O, Montecucco C (2006) Reversible skeletal neuromuscular paralysis induced by different lysophospholipids. *FEBS Lett* 580:6317-6321

Caccin P, Rossetto O, Montecucco C (2009) Neurotoxicity of inverted-cone shaped lipids. *Neurotoxicology* 30(2):174-81

Ceccarelli B, Hurlbut WP, Mauro A (1972) Depletion of vesicles from frog neuromuscular junctions by prolonged tetanic stimulation. *J Cell Biol* 54:30-38

Chang CC, Lee CY (1963) Isolation of neurotoxins from the venom of *Bungarus multicinctus* and their modes of neuromuscular blocking action. *Arch Int Pharmacodyn Ther* 144:241-57

Chen IL, Lee CY (1970) Ultrastructural changes in the motor nerve terminals caused by beta-bungarotoxin. *Virchows Arch B Cell Pathol* 6:318-325

Chang CC, Chen TF, Lee CY (1973) Studies of the presynaptic effect of beta-bungarotoxin on neuromuscular transmission. *J Pharmacol Exp Ther* 184(2):339-45

Chang CC, Huang MC, Lee CY (1973) Mutual antagonism between botulinum toxin and -bungarotoxin. *Nature* 243:166-167

Cull-Candy SG, Fohlman J, Gustavsson D, Lüllmann-Rauch R, Thesleff S (1976) The effects of taipoxin and notexin on the function and fine structure of the murine neuromuscular junction. *Neuroscience* 1(3):175-80

Dodds DC, Omeis IA, Cushman SJ, Helms JA, Perin MS (1997) Neuronal pentraxin receptor, a novel putative integral membrane pentraxin that interacts with

neuronal pentraxin 1 and 2 and taipoxin-associated calcium-binding protein 49. *J Biol Chem* 272:21488-21494

Fohlman J, Eaker D, Karlsoon E, Thesleff S (1976) Taipoxin, an extremely potent presynaptic neurotoxin from the venom of the australian snake taipan (*Oxyuranus s. scutellatus*). Isolation, characterization, quaternary structure and pharmacological properties. *Eur J Biochem* 68(2):457-69

Fohlman J, Eaker D, Dowdall MJ, Lüllmann-Rauch R, Sjödin T, Leander S (1979) Chemical modification of taipoxin and the consequences for phospholipase activity, pathophysiology, and inhibition of high-affinity choline uptake. *Eur J Biochem* 94(2):531-40

Georgieva DN, Perbandt M, Rypniewski W, Hristov K, Genov N, Betzel C. (2004) The X-ray structure of a snake venom Gln48 phospholipase A2 at 1.9A resolution reveals anion-binding sites. *Biochem Biophys Res Commun* 316(1):33-8

Gutiérrez JM, Theakston RDG, Warrell DA (2006) Confronting the neglected problem of snake bite envenoming: the need for a global partnership. *PLoS Med* 3:727-731

Halpert J, Eaker D (1975) Amino acid sequence of a presynaptic neurotoxin from the venom of *Notechis scutatus scutatus* (Australian tiger snake) *J Biol Chem*. 250(17):6990-7.

Hendon RA, Fraenkel-Conrat H (1971) Biological roles of the two components of crotoxin. *Proc Natl Acad Sci U S A* 68(7):1560-3

Herkert M, Shakhman O, Schweins E, Becker CM (2001) Beta-bungarotoxin is a potent inducer of apoptosis in cultured rat neurons by receptor-mediated internalization. *Eur J Neurosci* 14(5):821-8

Kamenskaya MA, Thesleff S (1974) The neuromuscular blocking action of an isolated toxin from the elapid (*Oxyuranus s. scutellatus*). *Acta Physiol Scand* 90:716-724

Kini RM (1997) Venom phospholipase A2 enzymes. John Wiley & Sons, Chichester

Kini RM, Evans HJ (1989) A model to explain the pharmacological effects of snake venom phospholipases A2. *Toxicon* 27:613-635

Kondo K, Toda H, Narita K (1978) Characterization of phospholipase A2 activity of beta1-bungarotoxin from *Bungarus multicinctus* venom. II. Identification of the histidine residue of beta1-bungarotoxin modified by p-bromophenacyl bromide. *J Biochem* 84(5):1301-8

Kuruppu S, Reeve S, Banerjee Y, Kini RM, Smith AI, Hodgson WC (2005) Isolation and pharmacological characterization of cannitoxin, a presynaptic neurotoxin from the venom of the Papuan Taipan (*Oxyuranus scutellatus canni*). *J Pharmacol Exp Ther* 315(3):1196-202

Kwong PD, McDonald NQ, Sigler PB, Hendrickson WA (1995) Structure of beta2-bungarotoxin: potassium channel binding by kunitz modules and targeted phospholipase action. *Structure* 3:1109-1119

Neco P, Rossetto O, Gil A, Montecucco C, Gutiérrez LM (2003) Taipoxin induces F-actin fragmentation and enhances release of catecholamines in bovine chromaffin cells. *J Neurochem* 85:329-337

Ng RH, Howard BD (1978) Deenergization of nerve terminals by beta-bungarotoxin. *Biochemistry* 17(23):4978-86

Pearson JA, Tyler MI, Retson KV, Howden ME (1991) Studies on the subunit structure of textilotoxin, a potent presynaptic neurotoxin from the venom of the Australian common brown snake (*Pseudonaja textilis*). 2. The amino acid sequence and toxicity studies of subunit D. *Biochim Biophys Acta* 1077(2):147-50

Petrovic U, Sribar J, Paris A, Rupnik M, Krzan M *et al*. (2004) Ammodytoxin, a neurotoxic secreted phospholipase A(2), can act in the cytosol of the nerve cell. *Biochem Biophys Res Commun* 324:981-985

Praznikar ZJ, Kovacic L, Rowan EG, Romih R, Rusmini P, Poletti A, Krizaj I, Pungercar J (2008) A presynaptically toxic secreted phospholipase A2 is internalized into motoneuron-like cells where it is rapidly translocated into the cytosol. *Biochim Biophys Acta* 1783(6):1129-39

Rigoni M, Schiavo G, Weston AE, Caccin P, Allegrini F *et al*. (2004) Snake presynaptic neurotoxins with phospholipase A2 activity induce punctate swellings of neurites and exocytosis of synaptic vesicles. *J Cell Sci* 117:3561-3570

Rigoni M, Caccin P, Gschmeissner S, Koster G, Postle AD *et al.* (2005) Equivalent effects of snake PLA2 neurotoxins and lysophospholipid-fatty acid mixtures. *Science* 310:1678-1680

Rigoni M, Pizzo P, Schiavo G, Weston AE, Zatti G *et al.* (2007) Calcium influx and mitochondrial alterations at synapses exposed to snake neurotoxins or their phospholipid hydrolysis products. *J Biol Chem* 282(15):11238-45

Rizzoli SO, Betz WJ (2005) Synaptic vesicle pools. *Nat Rev Neurosci* 6:57-69

Rossetto O, Montecucco C (2008) Presynaptic neurotoxins with enzymatic activities. *Handb Exp Pharmacol* 184:129-70

Rugolo M, Dolly JO, Nicholls DG (1986) The mechanism of action of beta-bungarotoxin at the presynaptic plasma membrane. *Biochem J* 233:519-523

Saul FA, Prijatelj-Žnidaršič P, Vulliez-le Normand B, Villette B, Raynal B, Pungerčar J, Križaj I, Faure G (2009) Comparative structural studies of two natural isoforms of ammodytoxin, phospholipases A(2) from *Vipera ammodytes ammodytes* which differ in neurotoxicity and anticoagulant activity. *J Struct Biol* [Epub ahead of print]

Simpson LL, Lautenslager GT, Kaiser II, Middlebrook JL (1993) Identification of the site at which phospholipase A2 neurotoxins localize to produce their neuromuscular blocking effects. *Toxicon* 31:13-26

Singh G, Gourinath S, Sharma S, Paramasivam M, Srinivasan A, Singh TP (2001) Sequence and crystal structure determination of a basic phospholipase A2 from common krait (Bungarus caeruleus) at 2.4 Å resolution: identification and characterization of its pharmacological sites. *J Mol Biol* 307(4):1049-59

Sribar J, Copic A, Paris A, Sherman NE, Gubensek F *et al*. (2001) A high affinity acceptor for phospholipase A2 with neurotoxic activity is a calmodulin. *J Biol Chem* 276:12493-12496

Sribar J, Copic A, Poljsak-Prijatelj M, Kuret J, Logonder U *et al.* (2003a) R25 is an intracellular membrane receptor for a snake venom secretory phospholipase A(2). *FEBS Lett* 553:309-314

Sribar J, Sherman NE, Prijatelj P, Faure G, Gubensek F *et al.* (2003b) The neurotoxic phospholipase A2 associates, through a non-phosphorylated binding

motif, with 14-3-3 protein gamma and epsilon isoforms. *Biochem Biophys Res Commun* 302:691-696

Theakston RDG, Warrell, DA, Griffiths E (2003) Report of a WHO workshop on the standardization and control of antivenoms. *Toxicon* 41: 541-557

Tyler MI, Barnett D, Nicholson P, Spence I, Howden ME (1987) Studies on the subunit structure of textilotoxin, a potent neurotoxin from the venom of the Australian common brown snake (*Pseudonaja textilis*). *Biochim Biophys Acta* 915(2):210-6

Westerlund B, Nordlund P, Uhlin U, Eaker D, Eklund H (1992) The three-dimensional structure of notexin, a presynaptic neurotoxic phospholipase A2 at 2.0 A resolution. *FEBS Lett* 301:159-164

2

SNAKE PHOSPHOLIPASE A2 NEUROTOXINS ENTER NEURONS, BIND SPECIFICALLY TO MITOCHONDRIA, AND OPEN THEIR TRANSITION PORE

THE JOURNAL OF BIOLOGICAL CHEMISTRY VOL. 283, NO. 49, pp. 34013–34020, December 5, 2008

Snake Phospholipase A_2 Neurotoxins Enter Neurons, Bind Specifically to Mitochondria, and Open Their Transition Pores*[S]

Received for publication, April 28, 2008, and in revised form, September 15, 2008 Published, JBC Papers in Press, September 22, 2008, DOI 10.1074/jbc.M803243200

Michela Rigoni[‡1], Marco Paoli[‡1], Eva Milanesi[§], Paola Caccin[‡], Andrea Rasola[‡], Paolo Bernardi[‡], and Cesare Montecucco[‡2]

From the [‡]Dipartimento di Scienze Biomediche Sperimentali, Università di Padova and Istituto di Neuroscienze del Consiglio Nazionale delle Ricerche, Viale Giuseppe Colombo 3, I-35121 Padova, Italy and the [§]Congenia Srl, Via Adamello 16, 20139 Milano, Italy

Snake presynaptic neurotoxins with phospholipase A_2 activity are potent inducers of paralysis through inhibition of the neuromuscular junction. These neurotoxins were recently shown to induce exocytosis of synaptic vesicles following the production of lysophospholipids and fatty acids and a sustained influx of Ca^{2+} from the medium. Here, we show that these toxins are able to penetrate spinal cord motor neurons and cerebellar granule neurons and selectively bind to mitochondria. As a result of this interaction, mitochondria depolarize and undergo a profound shape change from elongated and spaghetti-like to round and swollen. We show that snake presynaptic phospholipase A_2 neurotoxins facilitate opening of the mitochondrial permeability transition pore, an inner membrane high-conductance channel. The relative potency of the snake neurotoxins was similar for the permeability transition pore opening and for the phospholipid hydrolysis activities, suggesting a causal relationship, which is also supported by the effect of phospholipid hydrolysis products, lysophospholipids and fatty acids, on mitochondrial pore opening. These findings contribute to define the cellular events that lead to intoxication of nerve terminals by these snake neurotoxins and suggest that mitochondrial impairment is an important determinant of their toxicity.

Two classes of neurotoxins can paralyze the neuromuscular junction through their enzymatic activity: (i) the clostridial neurotoxins, metalloproteases acting specifically on SNARE (soluble NSF attachment protein receptor) proteins to cause tetanus and botulism, and (ii) the SPANs (1). SPANs[3] play a major role in envenomation and cause a botulism-like flaccid paralysis with autonomic symptoms (2, 3). The enzymatic activity and the neurospecificity make these toxins very effective; however, like botulinum neurotoxins, SPANs do not affect the cell body and axon of the motor neuron, allowing complete recovery in most patients (4).

Impairment of neuromuscular transmission by SPANs is traditionally measured in nerve-muscle preparations isolated from the mouse hemidiaphragm or from the chicken biventer cervicis. A simpler and more sensitive assay, based on SPAN-induced irreversible bulging of nerve terminals in culture, was recently described (5). It was also shown that an early consequence of the action of SPANs is the hydrolysis of phosphatidylcholine into lysophosphatidylcholine and fatty acids and that their equimolar mixture mimics the swelling response of nerve terminals to the toxin itself (6). The SPAN-induced nerve bulges accumulate Ca^{2+}, and, this event is accompanied by mitochondrial rounding and depolarization (7). The cytosolic [Ca^{2+}] increase could also trigger the activity of many Ca^{2+}-activated hydrolases of nucleic acids, proteins, and lipids, all factors that could account for the pronounced degeneration of nerve terminals poisoned by SPANs (8–11).

Previous studies indicated that SPANs can gain access to the cell interior. Indeed, fluorescein-conjugated β-Btx was found to rapidly enter hippocampal neurons in culture and was suggested to associate at least in part with lysosomes (12). By antibody labeling, Tpx was found to localize inside chromaffin cells in culture (13). Fluorophore-conjugated ammodytoxin A (a 14-kDa PLA_2 neurotoxin isolated from the venom of *Vipera ammodytes*) was detected in the nucleus of hippocampal neurons (14) and in the cytosol of undifferentiated NSC34 cells (15), a mouse neuroblastoma × spinal cord hybrid cell line (16). In addition, Tpx was reported to bind an endoplasmic reticulum-located protein *in vitro* (17), and ammodytoxin A was found to bind a variety of cytosolic proteins (18, 19) and R25, an integral protein of mitochondria (20). As SPANs require Ca^{2+} for their hydrolytic activity, the biological relevance of these findings was considered to be questionable. However, we recently documented that SPANs do induce the accumulation of Ca^{2+} within nerve terminals (7), and this finding reopened the possibility of a contribution of the entry of SPANs in the nerve terminal cytosol to the pathogenesis of envenomation.

* This work was supported in part by Telethon Grants GGP06133 and GGP04113, the Fondazione Cariparo Progetto "Physiopathology of the Synapse: Neurotransmitters, Neurotoxins and Novel Therapies" (to C. M.), and by the Ministero dell' Università e della Ricerca (to P. B.). The costs of publication of this article were defrayed in part by the payment of page charges. This article must therefore be hereby marked "*advertisement*" in accordance with 18 U.S.C. Section 1734 solely to indicate this fact.

[S] The on-line version of this article (available at http://www.jbc.org) contains supplemental Tables S1 and S2.

[1] Both authors contributed equally to this work.

[2] To whom correspondence should be addressed. Fax: 39-49-827-6049; E-mail: cesare.montecucco@unipd.it.

[3] The abbreviations used are: SPANs, snake presynoptic phospholipase A_2 neurotoxins; β-Btx, β-bungarotoxin; PTP, permeability transition pore; CGNs, cerebellar granular neurons; CRC, calcium retention capacity; CsA, cyclosporin A; mLysoPC, 1-myristoyllysophosphatidylcholine; Ntx, notexin; PLA_2, phospholipase A_2; OA, oleic acid; SCMNs, spinal cord motor neurons; Tpx, taipoxin; Tetx, textilotoxin.

Here, we report that active fluorescent derivatives of Ntx, β-Btx, and Tpx enter nerve terminals and bind specifically to mitochondria, whose morphology changes from the elongated, spaghetti-like shape to a rounded one. Rounded mitochondria were detected inside the toxin-induced bulges of nerve terminals. To understand the mechanistic basis for the mitochondrial changes, we investigated the effect of these neurotoxins on isolated mitochondria and discovered that SPANs are inducers of the mitochondrial PTP, with a relative potency that matches their PLA_2 activity. These findings have important consequences in defining the molecular events that lead to the pathogenesis of peripheral nerve paralysis caused by snake presynaptic PLA_2 neurotoxins in general.

EXPERIMENTAL PROCEDURES

Neurotoxins and Lipid Mixture Preparation—Ntx, Tpx, and Tetx were purchased from Venom Supplies; fluorescein isothiocyanate-conjugated β-Btx and β-Btx were from Sigma. Their purity was controlled by SDS-PAGE. 1-Myristoyllysophosphatidylcholine (mLysoPC; Sigma) and an oleic acid (OA; Sigma) mixture (mLysoPC + OA) were prepared as described previously (6).

Toxin Labeling and Assay—One hundred and fifty micrograms of purified toxin (Ntx, Tpx, and Tetx) were resuspended in 150 μl of 10 mM Hepes, 150 mM NaCl, pH 7.4; the pH of the reaction buffer was adjusted to 8.0 by adding sodium bicarbonate. Fifteen micrograms of Alexa568 dye (Molecular Probes) (from a stock solution of 10 μg/μl in Me_2SO) were added to the toxin solution. The reaction was carried out in the dark at room temperature for 1 h under continuous stirring and was stopped by the addition of 15 μl of 1.5 M hydroxylamine, pH 8.5. Excess dye was removed by extensive dialysis against 10 mM Hepes, 150 mM NaCl, pH 7.4 (Slide-A-Lyzer dialysis cassette, 10-kDa cut-off, Pierce). The conjugate was collected; its absorbance spectrum was recorded; and ratios of 0.5 Alexa568/Ntx molecule, of 1.2 Alexa568/Tpx molecule, and 3.5 Alexa568/Tetx molecule were determined. The toxicity of Alexa568-conjugated toxins was assayed in the mouse nerve-hemidiaphragm preparation as before (6). The fluorescent Ntx and Tpx derivatives, as well as the fluorescein isothiocyanate-conjugated β-Btx, were nearly as neurotoxic as their nonconjugated counterparts (supplemental Table S1). Alexa568-Tetx showed pronounced absorption onto the polylysine/polyornithine-laminin coating of the neuronal cultures and could not be used for neuron imaging.

Chemical Modifications of Notexin—Acetylation of lysine residues with acetic anhydride (Sigma) was performed as described (21) with minor modifications. Briefly, 30 μg of Ntx were dissolved in 100 μl of a saturated solution of sodium acetate in 50 mM sodium borate buffer, pH 8.2, and then cooled in an ice-water bath. The solution was treated with a total amount of 15 μl of a 1:500 dilution of acetic anhydride, distributed over five additions during 1 h at 4 °C. Acetylated Ntx was then dialyzed against 150 mM NaCl, 10 mM Hepes, pH 7.4 (Slide-A-Lyzer dialysis cassette), and conjugated with Alexa568 as described above.

Histidine modifications of Ntx with diethyl pyrocarbonate (Sigma) or *p*-bromophenacyl bromide (Sigma) were performed as described previously (22, 23). In the case of modification with diethyl pyrocarbonate, the reaction was performed in 50 mM phosphate buffer, pH 7.8, at 25 °C (toxin concentration = 0.2 mg/ml) by adding aliquots of a freshly prepared solution of diethyl pyrocarbonate in anhydrous ethanol. The reaction was followed by monitoring the absorbances at 243 and 278 nm in a Perkin-Elmer Lambda 5 spectrophotometer (22) and was stopped by the addition of imidazole (5 mM final concentration). The modified toxin was then dialyzed against 50 mM phosphate buffer, pH 7.0.

Notexin histidines were modified also with *p*-bromophenacyl bromide. Briefly, 100 μg of Ntx were resuspended in 100 μl of conjugation buffer (0.1 M sodium cacodylate-HCl, pH 6, 0.1 M NaCl). Incubation with *p*-bromophenacyl bromide was carried out at 30 °C at a molar reagent:protein ratio of 5:1 for 7 h and was followed by extensive dialysis against 10 mM Hepes, pH 7.4, 150 mM NaCl. Neurotoxicity, PLA_2 activity, and effects on isolated brain mitochondria of modified toxins were tested (supplemental Table S2).

Cell Culture Preparation—Rat CGNs were prepared from 6-day-old Wistar rats as described previously (24) and used 6–8 days after plating. Primary rat SCMNs were isolated from Sprague-Dawley (embryonic day 14) rat embryos and cultured following previously described protocols (25, 26). SCMNs were used after 5–8 days of neuronal differentiation *in vitro*.

Fluorescence Cell Imaging—SCMNs or CGNs were grown on 24-mm diameter coverslips and exposed to Alexa568-Tpx or Alexa568-Ntx or fluoresceinated β-Btx (25–50 nM) for different time periods at 37 °C in E4 medium (in the case of SCMNs) or Krebs-Ringer Hepes buffer (in the case of CGNs). E4 composition was 120 mM NaCl, 3 mM KCl, 2 mM $MgSO_4$, 2 mM $CaCl_2$, 10 mM glucose, and 10 mM Hepes, pH 7.4. Krebs-Ringer Hepes buffer composition was 125 mM NaCl, 5 mM KCl, 1.2 mM $MgSO_4$, 2 mM $CaCl_2$, 1.2 mM KH_2PO_4, 6 mM glucose, and 25 mM Hepes, pH 7.4. After incubation, cells were extensively washed with the same buffers, and the coverslips were placed on the stage of an inverted epifluorescence microscope (Leica ADMIRE3) equipped with a Leica DC500 CCD camera, 63× oil immersion objective (NA 1.4). Images were acquired using Leica FW4000 software and analyzed with Leica Deblur and ImageJ v1.35 software. For colocalization studies, neurons were loaded with the mitochondrial dye nonyl acridine orange (5 nM, Molecular Probes) for 30 min at 37 °C and then washed and incubated with the fluorescent toxins. Images were acquired at different times from toxin addition, and the fluorescent signals were superimposed.

PLA_2 Activity—The enzymatic activity of the four SPANs was measured with a commercial kit based on the use of the 1,2-dithio analogue of diheptanoylphosphatidylcholine as substrate (Cayman Chemicals). The hydrolysis of the thioester bond at the *sn*-2 position by PLA_2 generates free thiols that interact with 5,5′-dithiobis(nitrobenzoic acid), leading to an increase in the absorbance at 405 nm. ΔA_{405} was measured with a Beckman SpectraCount.

Rat Brain Mitochondrial Preparation—Two adult Wistar rat forebrains were used for each mitochondrial preparation. Rats were killed by cervical dislocation, and forebrains were immediately transferred to ice-cold isolation medium (250 mM

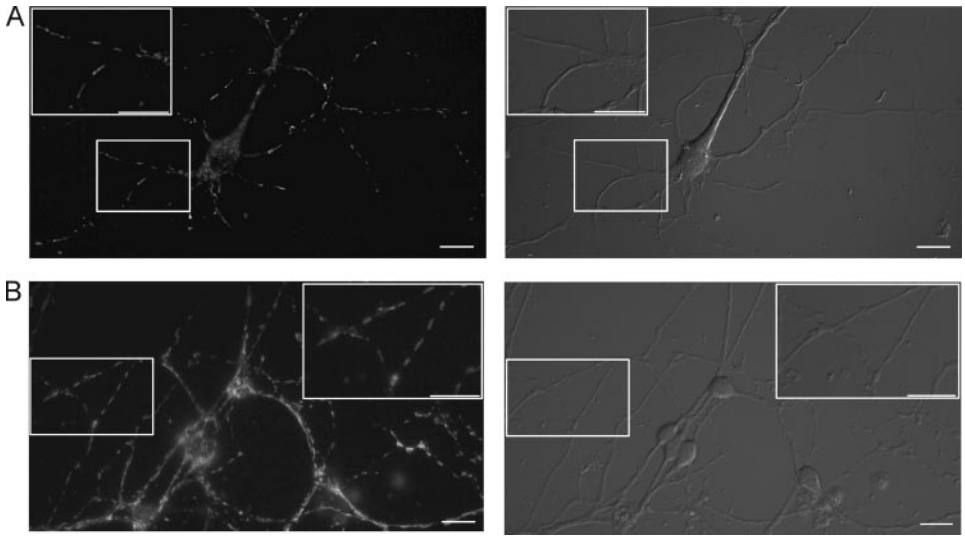

FIGURE 1. **Intracellular localization of SPANs in different primary neuronal cultures.** *A*, *left panel*: the intracellular distribution of Alexa568-Ntx in spinal cord motor neurons after a 5-min incubation at 37 °C (50 nM) is shown. *Right panel*: the corresponding bright field is shown. The *insets* show selected areas at higher magnitude. *Scale bar* = 10 μm. *B*, a similar intracellular distribution was found also in cerebellar granular neurons and with another SPAN, *i.e.* Alexa568-Tpx. *Scale bar* = 2 μm.

sucrose, 10 mM Tris-HCl, pH 7.4, 0.1 mM EGTA). Dissected forebrains were chopped with scissors and homogenized with 5–7 strokes of a loose-fitting Wheaton pestle. The homogenate was centrifuged for 3 min at 2,000 × *g* in isolation medium + 0.5% bovine serum albumin to precipitate the nuclei, and the supernatant was centrifuged twice for 8 min at 12,000 × *g*. The resulting pellet was resuspended in isolation medium without bovine serum albumin and centrifuged for 8 min at 12,000 × *g*. The resulting pellet was finally resuspended in isolation buffer to a protein concentration of 50–60 mg/ml. Protein concentration was quantified with the biuret assay.

Assessment of Permeability Transition in Isolated Mitochondria—Onset of the permeability transition was monitored as the fast Ca^{2+} release following accumulation of multiple 10 μM Ca^{2+} pulses at 1-min intervals (27). Extra-mitochondrial Ca^{2+} concentration was monitored with the Ca^{2+} indicator Calcium Green-5N (excitation/emission, 505/535 nm, Invitrogen) with a PerkinElmer 650–40 fluorescence spectrometer. Mitochondria were resuspended to a final protein concentration of 1 mg/ml in 2 ml of the following medium: 120 mM KCl, 10 μM EGTA, 5 mM glutamate, 2.5 mM malate, 1 mM Tris phosphate, 10 mM Tris-HCl, pH 7.4, 1 μM Calcium Green-5N. A quartz cuvette with continuous stirring through a magnetic bar was employed to ensure rapid mixing. The number of 10 μM Ca^{2+} pulses retained by the mitochondrial suspension before PTP opening was counted and set to 100% mitochondrial CRC. Similar experiments were carried out in the presence of the indicated toxins at concentrations ranging between 0.5 and 50 nM. Where indicated, 0.8 μM CsA (Sigma) was added to inhibit the opening of the PTP. CRC experiments were performed within 3 h of mitochondria isolation.

RESULTS

Snake Presynaptic PLA_2 Neurotoxins Enter Nerve Terminals—To obtain results of rather general value, we have used here four different SPANs and two different primary neuronal cultures. Alexa568 fluorescent derivatives of three SPANs with different quaternary structure, Ntx (monomeric, 14 kDa), Tpx (trimeric, 42 kDa), and Tetx (pentameric, 70 kDa), were prepared and their toxicities were tested. In the case of β-Btx (heterodimeric, 21 kDa) we used a commercial fluoresceinated toxin. The fluorescent derivatives were nearly as active as the native toxins; however, Alexa568-Tetx was strongly absorbed by the culture plate coating and could not be used for fluorescence imaging (see "Experimental Procedures"). Because the end plates of motor neurons *in vivo* are not readily accessible to investigation, we have studied the entry of fluorescent toxins in primary cultures of SCMNs, which are closer to peripheral motor neurons (26), and in a very homogeneous population of CGNs.

Fig. 1*A* shows that Alexa568-Ntx rapidly entered neuronal projections of SCMNs. Remarkably, fluorescent neurotoxin was not homogeneously distributed in the cytosol but rather localized to elongated, spaghetti-like structures that are clearly reminiscent of mitochondria. A similar staining pattern was found also in cerebellar granular neurons and with Alexa568-Tpx (Fig. 1*B*) and fluoresceinated β-Btx (data not shown), indicating that the mitochondrial-like staining is a rather general feature of SPANs.

With time, SPANs induce bulging of neuronal projections (5). Fig. 2 shows the staining of SCMNs with Alexa568-Tpx at 30 min; similar patterns were obtained with fluorescent Ntx and β-Btx (data not shown). The shape of the structures stained by the toxin changed during intoxication, and after 30 min, labeled organelles appeared as rounded bodies, which were always localized inside toxin-induced bulges.

SPANs Bind Specifically to Mitochondria within Neurons—The identification of the intracellular organelles stained by these neurotoxins as mitochondria is supported by the findings of Fig. 3, which shows a close superimposition between the staining patterns of Alexa568-Tpx and the mitochondrial dye nonyl acridine orange in SCMNs. Similar findings were obtained in CGNs and with fluorescent β-Btx and Ntx (data not shown). This latter observation is only apparently different from that of Herkert *et al.* (12) in hippocampal neurons, which was interpreted as partial localization of fluoresceinated β-Btx to lysosomes. In fact, a close inspection of the figures shows that the spotty distribution found in the neuronal projections is compatible with a staining of mitochondria after 30 min of incubation with the neurotoxin (see below). These observations are consistent with the electron microscopy pictures of motor neurons and CGNs exposed to these neurotoxins (3, 7–11, 28), whose mitochondria

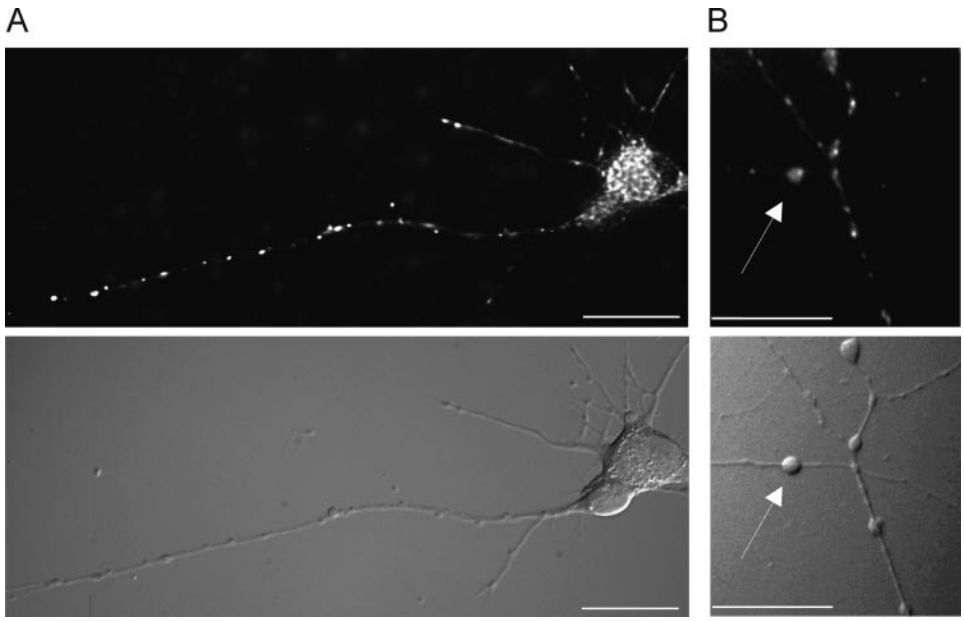

FIGURE 2. **Accumulation of SPAN staining within toxin-induced membrane enlargements with time.** Spinal cord motor neurons were incubated with 50 nM Alexa568-Tpx for 30 min at 37 °C and washed, and images were acquired. Alexa568-Tpx fluorescent signal accumulates within the toxin-induced membrane bulges, which can be better appreciated in *B*. The same results were obtained in cerebellar granular neurons and after Alexa568-Ntx and fluoresceinated β-Btx exposure (not shown). *Scale bar* = 10 μm in *A* and 5 μm in *B*.

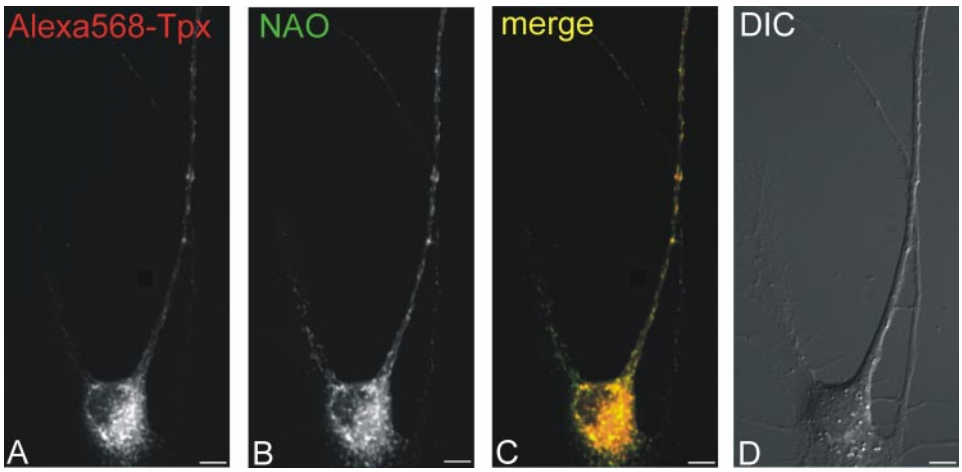

FIGURE 3. **Colocalization between SPANs and mitochondria.** Spinal cord motor neurons were incubated with 50 nM Alexa568-Tpx and 5 nM nonyl acridine orange (NAO) for 30 min at 37 °C and washed, and images were acquired. *A* and *B* show the fluorescence images at the single excitation wavelengths. *C* shows the superimposition between the two emitted wavelengths; *D* represents the corresponding differential interference contrast (*DIC*). *Scale bar* = 5 μm.

show rounding and alteration of cristae indicative of their loss of function.

The action of SPANs is known to be very specific for the presynaptic nerve terminals *in vivo*. Also in our cultures SPANs staining appears to be very specific for mitochondria within neurons, as shown by lack of toxin staining in non-neuronal cells (Fig. 4). These findings prompted us to investigate the effects of SPANs in mitochondria isolated from rat brain.

SPANs Open the Mitochondrial Permeability Transition Pore—A common cause of mitochondrial swelling and depolarization *in situ* is the opening of the mitochondrial PTP, an inner membrane high-conductance channel that can be desensitized by CsA (29). The propensity of the PTP to open in a population of mitochondria can be monitored with a sensitive technique based on the CRC, *i.e.* the amount of Ca^{2+} that can be taken up by mitochondria in the presence of inorganic phosphate before onset of PTP opening (27). Untreated, control mitochondria accumulated 10 pulses of 10 μM Ca^{2+} before onset of the permeability transition, which is readily detected by a precipitous release of the previously accumulated Ca^{2+} (Fig. 5*A*). Addition of as little as 1 nM Ntx dramatically decreased the threshold for PTP opening, which was observed after accumulation of three pulses of Ca^{2+} (Fig. 5*B*). It should be noted that prior to PTP opening, the rate of Ca^{2+} uptake in Ntx-treated mitochondria was indistinguishable from that of controls, indicating that, in the absence of added Ca^{2+}, Ntx does not affect energy coupling. As expected for a PTP-dependent event, treatment with CsA increased the CRC both in the absence (Fig. 5*C*) and presence (Fig. 5*D*) of Ntx.

We then investigated the effects of the four SPANs on the CRC and their relative potency. Ntx was the most effective, β-Btx and Tpx displayed an intermediate PTP sensitizing activity, whereas Tetx was nearly ineffective (Fig. 6*A*). This order of potency correlates well with the PLA_2 activity of the four SPANs measured by an *in vitro* assay (Ntx, 371 μmol/min/mg; β-Btx, 218 μmol/min/mg; Tpx, 100 μmol/min/mg; Tetx, 10 μmol/min/mg; see "Experimental Procedures").

To test the hypothesis that the enzymatic activity is indeed responsible for facilitation of PTP opening by SPANs, we determined the direct effect of the products of the PLA_2 activity, mLysoPC, and OA. These were added to rat brain mitochondria either individually or in the 1:1 molar mixture that is produced by SPANs (Fig. 6*B*). Consistent with our hypothesis, the equimolar mixture of mLysoPC + OA (1 μM) facilitated PTP opening, whereas mLysoPC alone was less effective. OA had a strong effect, in line with previous observations, demonstrating that fatty acids (*i.e.* arachidonic and palmitic) are effective inducers of the PTP in isolated mitochondria and intact cells (30). Together with our previous findings that fatty acid alone has a minor inhibitory effect on the transmission of the nerve impulse to the muscle (6), the present result indicates that very little fatty acid is able to partition from the plasma membrane

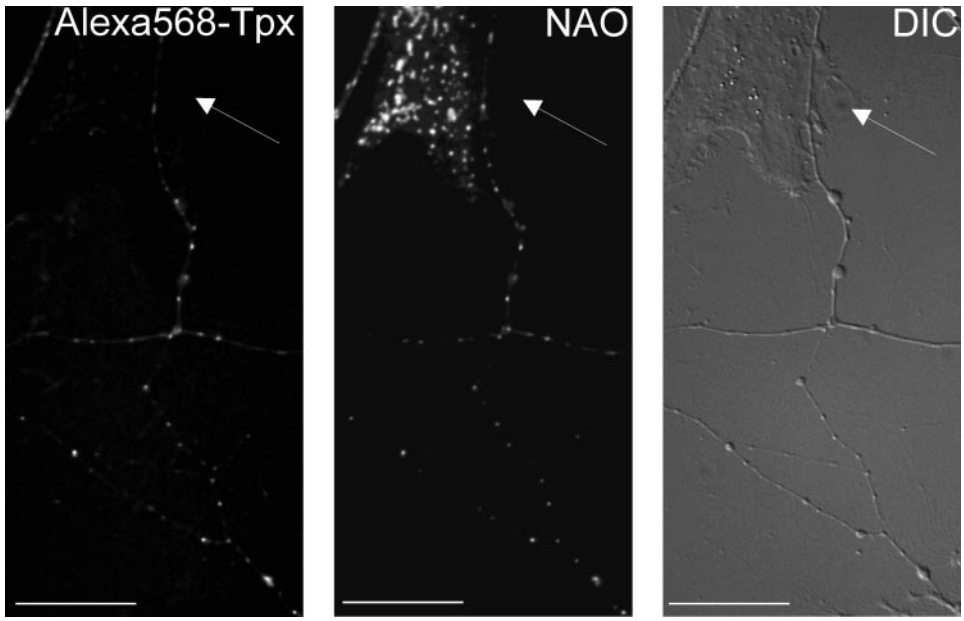

FIGURE 4. **SPANs specifically localize within neurons.** Alexa568-Tpx (25 nM) intracellular localization in primary cultures of spinal cord motor neurons after a 30 min incubation at 37 °C is confined to neuronal cells, as demonstrated by the lack of fluorescent signal in fibroblasts, whose mitochondria are stained well with nonyl acridine orange (*NAO*). *Scale bar* = 5 μM. *DIC*, differential interference contrast.

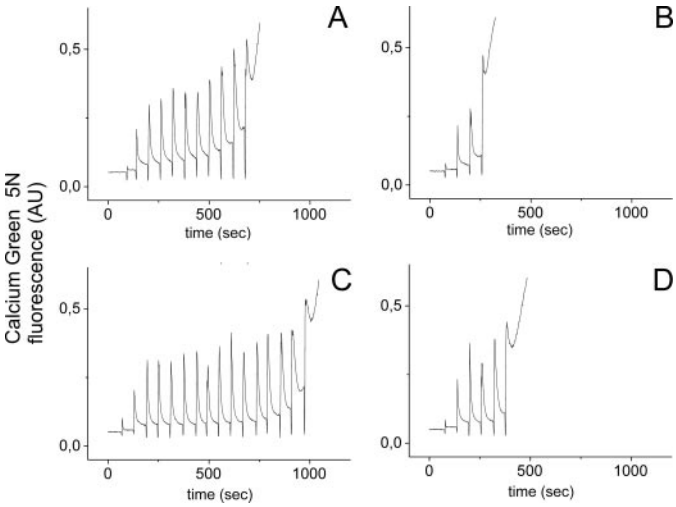

FIGURE 5. **Influence of Ntx and CsA on mitochondrial CRC.** Purified mitochondria were resuspended in the presence of Calcium Green-5N as described under "Experimental Procedures," and CRC was tested. At 60-s intervals, 10 μM Ca^{2+} pulses were added until occurrence of the permeability transition, which is marked by a fast release of the previously accumulated Ca^{2+}. *A* and *B*, reduced mitochondrial CRC in Ntx-treated mitochondria (*B*, 1 nM) compared with control (*A*). *C* and *D*, the ability of CsA to delay mitochondrial Ca^{2+} release of control (*C*) and Ntx-treated mitochondria (*D*, 1 nM). *AU*, arbitrary units.

into the mitochondria of the nerve terminals after its release by the PLA_2 activity of these neurotoxins. Further evidence that the PLA_2 enzymatic activity of the SPANs is instrumental in inducing the mitochondrial change in permeability was obtained in experiments performed with chemically inactivated Ntx. The toxin was acetylated, and this derivative retained 2.9 ± 2.5% of the PLA_2 activity of the unmodified toxin ($n = 3$). Acetylated Ntx did not significantly inhibit neurotransmission of the mouse hemidiaphragm preparation, did not stain or induce any bulging of neurons in culture, and failed to induce opening of the mitochondrial PTP. Notexin was also chemically modified with the histidine-specific reagents diethyl pyrocarbonate and *p*-bromophenacyl bromide following established procedures (22, 23), which led to partial loss of PLA_2 activity (supplemental Table S2). Importantly, the percentage of loss of enzymatic activity correlated well with the percentages of loss of neurotoxicity and of capability of opening the mitochondrial PTP. These data strongly support the proposal that the PLA_2 activity of SPANs is involved in their effect on the mitochondrial PTP.

Fig. 7 reports the relative protective effect of the PTP inhibitor CsA in the absence or presence of the four SPANs. This parameter has similar values whether or not a SPAN was present, whichever SPAN is considered. This indicates that SPANs do not directly permeabilize the mitochondrial membrane, with ensuing unspecific Ca^{2+} leak. On the other hand, the effect of SPANs appears to be rather specific for the PTP channel, as CsA inhibited the effect of the toxins to a similar extent, with relative values close to those of the controls.

DISCUSSION

The main findings of the present study are (i) presynaptic snake neurotoxins of different size (from 14 to 42 kDa) endowed with PLA_2 activity enter neurons within a short time of addition; (ii) they bind specifically to mitochondria and induce a shape change within regions of nerve terminals that undergo swelling to form round bulges of the plasma membrane; and (iii) these neurotoxins induce opening of the mitochondrial PTP, which leads to release of Ca^{2+}, with an order of potency that matches their PLA_2 enzymatic activities.

The entry of SPANs inside cells was reported before. β-Btx and ammodytoxin A were detected within hippocampal neurons (12, 14), ammodytoxin A was recently found also in NSC34 cells (15), and Tpx staining by antibody labeling was reported within chromaffin cells (13). It was also previously established that endocytosis inside acidic intracellular compartments, as is the case of botulinum neurotoxins, is not involved in the intoxication by SPANs (31). The recent observation that ammodytoxin A localizes inside vesicles in the cytosol of undifferentiated NSC34 cells may be due to tumor transformation itself and/or to the fact that the cells used were not differentiated and had no neuronal appearance (15). Although toxin endocytosis cannot be excluded, the early detection of SPANs inside the cell cytosol is not consistent with the time course of endocytosis. We are left with the possibility that SPANs enter directly by crossing the plasma membrane. It is not known whether this is an intrinsic property of these molecules or whether an initial

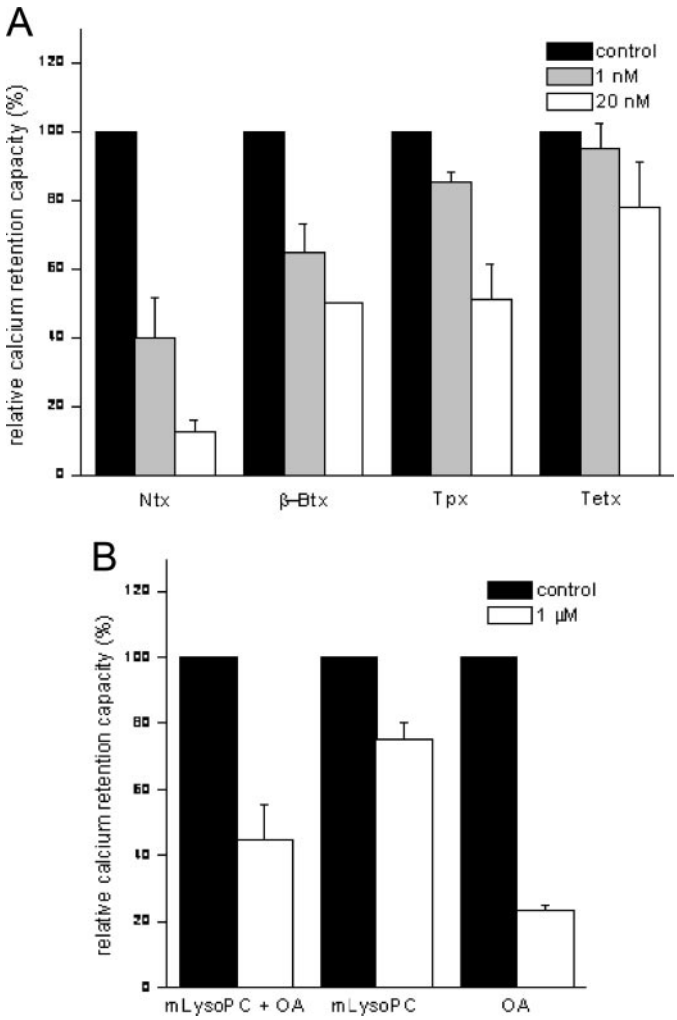

FIGURE 6. **Effect of SPANs and PLA_2 activity products at different concentrations on Ca^{2+} uptake of purified rat brain mitochondria.** *A*, mitochondria were resuspended as described under "Experimental Procedures," and CRC was tested in the presence of the four snake neurotoxins at high (20 nM, *white bars*) and low (1 nM, *gray bars*) concentrations. CRC decrease of toxin-treated mitochondria is concentration-dependent. *B*, the hydrolytic products of PLA_2 activity (mLysoPC and OA) were tested both alone or in an equimolar mixture (1 μM). Data represent mean CRC values of intoxicated mitochondria normalized to control samples (*black bars*). For each condition, trials were performed in triplicate.

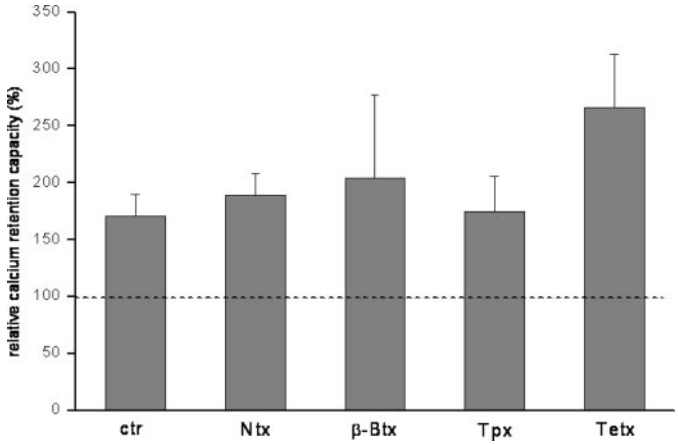

FIGURE 7. **Delayed SPAN-induced PTP opening by CsA.** Calcium retention capacity of control and SPAN-treated (20 nM) mitochondria was measured in the absence or presence of CsA (0.8 μM). CRC values of CsA-treated mitochondria (in the absence or presence of toxins, respectively) are normalized to those of samples not treated with CsA (*dotted line*). An increased threshold for PTP opening is observed for both control and SPAN-treated mitochondria. For each condition, trials were performed in triplicate.

hydrolysis of the phospholipids of the outer layer of the plasma membrane is a prerequisite for their entry. The finding that Sr^{2+}, which does not sustain the PLA_2 activity of SPANs, inhibited ammodytoxin A entry supports the latter possibility (15). Also, the present finding that PLA_2 inactivation of Ntx leads to loss of neurotoxicity and loss of effect on mitochondria is consistent with this possibility.

Here, we report the first evidence that SPANs inside neurons bind to mitochondria and induce their change of shape from the physiological elongated to the rounded, swollen form, which is observed in many pathological states. Given that the entry of SPANs inside excitatory cells was already reported (12–15), why was their specific binding to mitochondria not detected before? A key issue is that the typical spaghetti-like staining is maintained for a very short time following toxin addition. Because mitochondrial rounding and impairment readily follow SPAN nerve terminal poisoning (7–9), the affected organelles are no longer easily identified as mitochondria. It is also possible that these neurotoxins bind efficiently to mitochondria only within neuronal cells, as suggested by the study of Ng and Howard (32), who found that β-Btx only affected brain mitochondria. This would explain why mitochondrial staining was not detected in chromaffin cells (13) and in undifferentiated NSC34 cells (15), but does not explain the lack of this type of staining in hippocampal neurons by ammodytoxin A (14). However, it should be considered that the fluorescent ammodytoxin A used in NSC34 cells displayed a 5-fold lower binding affinity for the mitochondrial R25 protein (15), suggesting that the toxin was significantly modified by the procedure used for fluorescent dye coupling, which may in turn have affected its subcellular interactions. As mentioned above, a re-inspection of hippocampal neurons intoxicated with β-Btx (12) is compatible with the mitochondrial staining found here. The mitochondrial binding of SPANs re-evaluates the biochemical finding that ammodytoxin A binds to a mitochondrial protein termed R25 (20), which could be involved as well in the mitochondrial interactions detected here in intact cells.

Bulging is the result of an excess of membrane accumulation and the positive curvature of the plasma membrane caused by the presence of lysophospholipids on the outer layer (1, 6, 33, 34). SPANs induce bulging in different neurons in culture, an event that was found to be associated with induced exocytosis and inhibition of the retrieval of synaptic vesicles (5–6, 35). The same phenotype is induced by the addition to neurons of the PLA_2 hydrolysis products (6). Interestingly, the mitochondrial shape changes in toxin-treated neurons take place within bulges of the neuronal projections and may well be caused by PTP opening mediated by the very same products of phospholipid hydrolysis. Accordingly, we found that the addition of an equimolar mixture of mLysoPC + OA induced the opening of the mitochondrial PTP (Fig. 6*B*).

The *in vivo* mitochondrial targeting of SPANs called for a reappraisal of their direct action on mitochondria, in light of the

current knowledge regarding the role of mitochondria in controlling the Ca^{2+} concentration of the cytosol (36, 37) as well as the fact that SPANs do induce a high increase of $[Ca^{2+}]$ within nerve terminals (7). It has long been known that Ntx and β-Btx affect isolated mitochondria and are capable of decreasing Ca^{2+} uptake by brain mitochondria and sarcoplasmic reticulum (32, 38). Our finding that SPANs sensitize the PTP to opening by Ca^{2+} readily provides an explanation for these previous observations, but also clarifies a novel and important aspect of the mitochondrial effects of SPANs. Indeed, our results demonstrate that (i) SPANs do not directly affect mitochondrial coupling or their Ca^{2+} uptake systems because the kinetics of mitochondrial Ca^{2+} uptake is not affected until the PTP opens, and (ii) Ca^{2+} release (and impairment of further Ca^{2+} uptake) is caused by PTP opening. This mitochondrial impairment caused by SPANs may then substantially worsen the deregulation of Ca^{2+} homeostasis. This sequence of events is entirely consistent with the observation that toxin-treated mitochondria are no longer able to buffer cytosolic Ca^{2+} and that they contribute to the triggering of an apoptotic program of cell death that was actually shown to occur in the hippocampal neurons exposed to the action of β-Btx (12).

Are the present findings relevant to the pathogenesis of envenomation by snakes whose venoms include SPANs as a major toxin component? As discussed in detail elsewhere (4, 11), available data suggest that blockade of peripheral nerve terminals with ensuing flaccid paralysis is mainly due to the SPAN-catalyzed hydrolysis of phospholipids of the presynaptic membrane, followed by massive entry of Ca^{2+}. Together, these two events would induce exocytosis of the synaptic vesicles of the affected nerve terminals not followed by endocytosis. It has been argued that the entry of SPANs inside the nerve cytosol must have a role (39). Clearly, much depends on the kinetics of entry. If the SPAN enters rapidly by itself, then it may begin to act as soon as the cytosolic Ca^{2+} concentration has risen to a level sufficient to support the PLA_2 activity. On the other hand, the inhibitory effect of Sr^{2+} mentioned above (15) and the inability to enter of the inactive acetylated Ntx indicate that SPANs may require phospholipid hydrolysis to alter the membrane in such a way as to promote their own translocation into the cytosol. Further investigations are needed to discriminate between these two possibilities.

In summary, we can safely conclude that the specific action of SPANs on the mitochondrial PTP channel well accounts for the rounding and swelling of mitochondria detected by all electron microscopy investigations of SPAN-intoxicated neurons (8–10, 28, 40–42). Our results provide a molecular explanation for these morphological observations and indicate that SPANs play a direct role not only in the blockade of nerve terminals, but also in the ensuing mitochondrial degeneration (8–11). The present findings call for detailed investigations of the kinetics of action of SPANs with an analysis of the various steps of intoxication, with particular attention to binding, entry into the cytosol, and effects on mitochondria.

Acknowledgment—We thank Dr. Valeria Petronilli for helpful advice.

REFERENCES

1. Rossetto, O., Morbiato, L., Caccin, P., Rigoni, M., and Montecucco, C. (2006) *J. Neurochem.* **97,** 1534–1545
2. Connolly, S., and Warrell, D. A. (1995) *Ann. Neurol.* **38,** 916–920
3. Prasarnpun, S., Walsh, J., Awad, S. S., and Harris, J. B. (2005) *Brain* **128,** 2987–2996
4. Rossetto, O., and Montecucco, C. (2008) *Handb. Exp. Pharmacol.* **184,** 129–170
5. Rigoni, M., Schiavo, G., Weston, A. E., Caccin, P., Allegroni, F., Pennuto, M., Valtorta, F., Montecucco, C., and Rossetto, O. (2004) *J. Cell Sci.* **117,** 3561–3570
6. Rigoni, M., Caccin, P., Gschmeissner, S., Koster, G., Postle, A. D., Rossetto, O., Schiavo, G., and Montecucco, C. (2005) *Science* **310,** 1678–1680
7. Rigoni, M., Pizzo, P., Schiavo, G., Weston, A. E., Zatti, G., Caccin, P., Rossetto, O., Pozzan, T., and Montecucco, C. (2007) *J. Biol. Chem.* **282,** 11238–11245
8. Cull-Candy, S. G., Fohlman, J., Gustavsson, D., Lullmann-Rauch, R., and Thesleff, S. (1976) *Neuroscience* **1,** 175–180
9. Gopalakrishnakone, P., and Hawgood, B. J. (1984) *Toxicon* **22,** 791–804
10. Dixon, R., and Harris, J. B. (1999) *Am. J. Pathol.* **154,** 447–455
11. Montecucco, C., Gutiérrez, J. M., and Lomonte, B. (2008) *CMLS Cell. Mol. Life Sci.* **65,** 2897–2912
12. Herkert, M., Shakhman, O., Schweins, E., and Becker, C. M. (2001) *Eur. J. Neurosci.* **14,** 821–828
13. Neco, P., Rossetto, O., Gil, A., Montecucco, C., and Gutiérrez, L. M. (2003) *J. Neurochem.* **83,** 329–337
14. Petrovic, U., Sribar, J., Paris, A., Rupnik, M., Krzan, M., Vardjan, N., Gubensek, F., Zorec, R., and Križaj, I. (2004) *Biochem. Biophys. Res. Commun.* **324,** 981–985
15. Pražnikar, Z. J., Kovačič, L., Rowan, E. G., Romih, R., Rumini, P., Poletti, A., Križaj, I., and Pungerčar, J. (2008) *Biochim. Biophys. Acta* **1783,** 1129–1139
16. Cashman, N. R., Durham, H. D., Blusztajn, J. K., Oda, K., Tabira, T., Shaw, I. T., Dahrouge, S., and Antel, J. P. (1992) *Dev. Dyn.* **194,** 209–221
17. Dodds, D., Schlimgen, A. K., Lu, S. Y., and Perin, M. S. (1995) *J. Neurochem.* **64,** 2339–2344
18. Sribar, J., Copic, A., Paris, A., Sherman, N. E., Gubensek, F., Fox, J. W., and Križaj, I. (2001) *J. Biol. Chem.* **276,** 12493–12496
19. Sribar, J., Sherman, N. E., Prijatelj, P., Faure, G., Gubensek, F., Fox, J. W., Aitken, A., Pungerčar, J., and Križaj, I. (2003) *Biochem. Biophys. Res. Commun.* **302,** 691–696
20. Sribar, J., Copic, A., Poljsak-Prijatelj, M., Kuret, J., Logonder, U., Gubensek, F., and Križaj, I. (2003) *FEBS Lett.* **553,** 309–314
21. Means, G. E., and Feeney, R. E. (1971) *Chemical Modification of Proteins*, p. 214, Holden-Day, Inc., San Francisco
22. Papini, E., Schiavo, G., Sandonà, D., Rappuoli, R., and Montecucco, C. (1989) *J. Biol. Chem.* **264,** 12385–12388
23. Halpert, J., and Karlsson, E. (1975) *FEBS Lett.* **61,** 72–76
24. Levi, G., Aloisi, F., Ciotti, M. T., and Gallo, V. (1984) *Brain Res.* **290,** 77–86
25. Arce, V., Garces, A., de Bovis, B., Filippi, P., Henderson, C. E., Pettmann, B., and de Lapeyriere, O. (1999) *J. Neurosci. Res.* **55,** 119–126
26. Bohnert, S., and Schiavo, G. (2005) *J. Biol. Chem.* **280,** 42336–42344
27. Fontaine, E., Ichas, F., and Bernardi, P. (1998) *J. Biol. Chem.* **273,** 25734–25740
28. Fohlman, J., Eaker, D., Dowdall, M. J., Lüllmann-Rauch, R., Sjödin, T., and Leander, S. (1979) *Eur. J. Biochem.* **94,** 531–540
29. Bernardi, P., Krauskopf, A., Basso, E., Petronilli, V., Blachly-Dyson, E., Di Lisa, F., and Forte, M. A. (2006) *FEBS J.* **273,** 2077–2099
30. Scorrano, L., Penzo, D., Petronilli, V., Pagano, F., and Bernardi, P. (2001) *J. Biol. Chem.* **276,** 12035–12040
31. Simpson, L. L., Coffield, J. A., and Bakry, N. (1994) *J. Pharmacol. Exp. Ther.* **269,** 256–262
32. Ng, R. H., and Howard, B. D. (1980) *Proc. Natl. Acad. Sci. U. S. A.* **77,** 1346–1350
33. Chernomordik, L. V., and Kozlov, M. M. (2003) *Annu. Rev. Biochem.* **72,** 175–207

34. Zimmerberg, J., and Kozlov, M. M. (2006) *Nat. Rev. Mol. Cell Biol.* **7,** 9–19
35. Bonanomi, D., Pennuto, M., Rigoni, M., Rossetto, O., Montecucco, C., and Valtorta, F. (2005) *Mol. Pharmacol.* **67,** 1901–1908
36. Giacomello, M., Drago, I., Pizzo, P., and Pozzan, T. (2007) *Cell Death Differ.* **14,** 1267–1274
37. Rasola, A., and Bernardi, P. (2007) *Apoptosis* **12,** 815–833
38. Wagner, G. M., Mart, P. E., and Kelly, R. B. (1974) *Biochem. Biophys. Res. Commun.* **58,** 475–481
39. Pungerčar, J., and Križaj, I. (2007) *Toxicon* **50,** 871–892
40. Lee, C. Y., Tsai, M. C., Chen, Y. M., Ritonja, A., and Gubensek, F. (1984) *Arch. Int. Pharmacodyn. Ther.* **268,** 313–324
41. Chen, I. L., and Lee, C. Y. (1970) *Virchows Arch. B Cell Pathol.* **6,** 318–325
42. Prasarnpun, S., Walsh, J., and Harris, J. B. (2004) *Neuropharmacology* **47,** 304–314

3

MASS SPECTROMETRY ANALYSIS OF THE PHOSPHOLIPASE A2 ACTIVITY OF SNAKE PRESYNAPTIC NEUROTOXINS IN CULTURED NEURONS

Journal of Neurochemistry

JOURNAL OF NEUROCHEMISTRY | 2009

doi: 10.1111/j.1471-4159.2009.06365.x

Mass spectrometry analysis of the phospholipase A_2 activity of snake pre-synaptic neurotoxins in cultured neurons

Marco Paoli,* Michela Rigoni,* Grielof Koster,† Ornella Rossetto,* Cesare Montecucco* and Anthony D. Postle†

*Department of Biomedical Sciences and CNR Institute of Neuroscience, University of Padova, Padova, Italy

†School of Medicine, University of Southampton, Southampton, UK

Abstract

Snake pre-synaptic phospholipase A_2 neurotoxins paralyse the neuromuscular junction by releasing phospholipid hydrolysis products that alter curvature and permeability of the pre-synaptic membrane. Here, we report results deriving from the first chemical analysis of the action of these neurotoxic phospholipases in neurons, made possible by the use of high sensitivity mass spectrometry. The time–course of the phospholipase A_2 activity (PLA_2) hydrolysis of notexin, β-bungarotoxin, taipoxin and textilotoxin acting in cultured neurons was determined. At variance from their enzymatic activities *in vitro*, these neurotoxins display comparable kinetics of lysophospholipid release in neurons, reconciling the large discrepancy between their *in vivo* toxicities and their *in vitro* enzymatic activities. The ratios of the lyso derivatives of phosphatidyl choline, ethanolamine and serine obtained here together with the known distribution of these phospholipids among cell membranes, suggest that most PLA_2 hydrolysis takes place on the cell surface. Although these toxins were recently shown to enter neurons, their intracellular hydrolytic action and the activation of intracellular PLA_2s appear to contribute little, if any, to the phospholipid hydrolysis measured here.

Keywords: lysophospholipids, phospholipase A_2 activity, snake neurotoxins, toxicity.

J. Neurochem. (2009) 10.1111/j.1471-4159.2009.06365.x

The venom of many Australian and Asiatic Elapid snakes is highly poisonous and the majority of the symptoms of envenomation in humans is the result of the action of neurotoxins endowed with phospholipase A_2 activity (PLA_2) activity, which are prominent components of these venoms (Chen and Lee 1970; Connolly *et al.* 1995; Harris *et al.* 2000; Prasarnpun *et al.* 2005). Human envenomation is a major health concern in many countries of the world (Gutiérrez *et al.* 2006). These neurotoxins are abbreviated here as snake pre-synaptic PLA_2 neurotoxins (SPANs). The role of their PLA_2 enzymatic activity in the blockade of the neuromuscular junction (NMJ) has been long debated (Rosenberg 1997; Kini 2003; Gutiérrez *et al.* 2006), but recent results demonstrated that their phospholipid hydrolysis products, lysophospholipids (LysoPLs) and fatty acids (FAs), are sufficient to cause NMJ paralysis with the associated pathological changes (Rigoni *et al.* 2005; Caccin *et al.* 2006). Therefore, to define the pathological action of SPANs it is necessary to analyse their PLA_2 activity *in vivo* as a function of time. Recent advances in mass spectrometry (MS) of lipids (Han and Gross 2003; Pulfer and Murphy 2003; Postle *et al.* 2007; Davis *et al.* 2008; Wilensky *et al.* 2008) have enabled us to analyse PLA_2 hydrolysis products with high sensitivity and specificity. Electrospray ionization (ESI)-MS, coupled with diagnostic tandem MS/MS scans, permits routine comprehensive characterization of membrane lipids from as few as 10^6 cells.

Received June 19, 2009; revised manuscript received August 4, 2009; accepted August 17 2009.

Address correspondence and reprint requests to Anthony D. Postle, Division of Infection, Inflammation and Immunity, School of Medicine, Southampton General Hospital, Southampton SO16 6YD, UK; E-mail: A.D.Postle@soton.ac.uk or to Cesare Montecucco, Department of Biomedical Sciences, University of Padova, Via G. Colombo 3, 35121 Padova, Italy; E-mail: cesare.montecucco@unipd.it

Abbreviations used: AA, aristolochic acid; β-Btx, β-bungarotoxin; CGNs, cerebellar granule neurons; ESI, electrospray ionization; FA, fatty acid; LysoPLs, lysophospholipids; LysoPC, lysophosphatidylcholine; LysoPE, lysophosphatidylethanolamine; MS, mass spectrometry; NMJ, neuromuscular junction; Ntx, notexin; PC, phosphatidylcholine; PE, phosphatidylethanolamine; PS, phosphatidylserine; PLA_2, phospholipase A_2 activity; SPANs, snake pre-synaptic PLA_2 neurotoxins; Tetx, textilotoxin; Tpx, taipoxin.

It is still impossible to analyse quantitatively the lipid products released by SPANs at the NMJ, their principal target in humans, for obvious technical reasons. However, it is well established that SPANs are highly toxic when injected into the CNS (Gandolfo *et al.* 1996; Kolko *et al.* 1999) and act on isolated brain-derived preparations (Rehm and Betz 1982; Nicholls *et al.* 1985; Rugolo *et al.* 1986). Therefore, data obtained with cultured CNS neurons were relevant and were as close to the *in vivo* situation as is currently experimentally possible. Methods are available to maintain many CNS neurons in primary cultures, but these cultures are mixtures of neurons and glial cells except for the granular neurons of the cerebellum (CGNs, cerebellar granule neurons), wherein cultures consist almost entirely of neurons (Lasher and Zaigon 1972; Levi *et al.* 1984). We have shown previously that SPANs are very active on these neurons (Rigoni *et al.* 2004). Using a pure neuronal culture is essential to achieve consistent and reliable MS analysis of changes in lipid compositions, as the presence of a large component of SPAN-resistant glial cells would dilute the changes induced by the toxins. Moreover, glial cells and neurons will have distinct and different compositions of membrane lipid, which will further complicate the MS analysis. CGN neurons are highly sensitive to SPANs and develop a well-defined bulging at axon and dendrite terminals within few minutes from toxin addition; such morphological alteration is accompanied by cytosolic calcium increase at nerve terminals and glutamate release from neurons (Rigoni *et al.* 2004, 2007). These effects are mimicked by the addition of an equimolar mixture of the PLA_2 hydrolysis products, lysophosphatidylcholine (LysoPC) + oleic acid, indicating that these molecules are the biochemical mediators of SPAN action (Rigoni *et al.* 2005; Caccin *et al.* 2006). Of the two lipid molecules, LysoPC was shown to be most effective (Caccin *et al.* 2006, 2009). We have shown previously that LysoPC is by far the major class of LysoPL released by two SPANs (Rigoni *et al.* 2005), but a comparative and detailed analysis of their kinetics of action including the other two major plasma membrane phospholipids [phosphatidylethanolamine (PE) and phosphatidylserine (PS)] is still lacking. To obtain results of rather general interest here, we have challenged CGN primary cultures with four different neurotoxic SPANs that differ in terms of quaternary structure and *in vitro* PLA_2 activity: notexin (Ntx), β-bungarotoxin (β-Btx), taipoxin (Tpx) and textilotoxin (Tetx). Ntx is a 14 kDa monomer, β-Btx is a heterodimer with one 14 kDa active PLA_2 subunit, Tpx is a trimer of similar 14 kDa subunits one of which is PLA2 active, and Tetx consists of five or six similar 14 kDa subunits, only one of which is enzymatically active (Montecucco and Rossetto 2008; Aquilina 2009). The results obtained provide the kinetics of phospholipid hydrolysis in a homogeneous population of neurons and strongly indicate the outer layer of the plasma membrane as their major site of phospholipid hydrolysis.

Materials and methods

Materials

Notexin, Tpx and Tetx were purchased from Venom Supplies (Tanuda, South Australia); β-Btx was obtained from Sigma (St. Louis, MO, USA). Their purity was controlled by sodium dodecyl sulfate–polyacrylamide gel electrophoresis. Aristolochic acid was supplied by BIOMOL Research Laboratories (Plymouth Meeting, PA, USA) and ionomycin by Calbiochem (San Diego, CA, USA). Phospholipid internal standards were obtained from Avanti Polar Lipids (Alabaster, AL, USA).

Cell cultures

Rat CGNs were prepared from 6-day-old Wistar rats as previously described (Levi *et al.* 1984) and plated at 2×10^6 cells per 35-mm Petri dish. Cells were used 6 days after plating. NSC34 cells were maintained in Dulbecco's modified Eagle's medium with sodium pyruvate, supplemented with 10% fetal bovine serum. Cells were plated at 4×10^4 cells per 35-mm Petri dish and differentiated for 5 days with 5% fetal bovine serum and 10 μM retinoic acid before intoxication.

PLA_2 activity

The enzymatic activity of the four SPANs was measured using the 1,2-dithio analogue of di-heptanoyl PC as substrate (Cayman Chemicals, Ann Arbor, MI, USA). The hydrolysis of the thio ester bond at the *sn*-2 position by PLA_2 generated free thiols that interacted with 5,5′-dithiobis-(2-nitrobenzoic acid), leading to an increase in absorbance at 405 nm (Reynolds *et al.* 1992). ΔA_{405} was measured with a Packard SpectraCount spectrophotometer (Packard, Chicago, IL, USA).

Lipid analysis

Cerebellar granule neurons (6 days *in vitro*) grown on 35-mm polylysine-coated Petri dishes (2×10^6 cells/dish) were extensively washed with pre-warmed Krebs–Ringer buffer (125 mM NaCl, 5 mM KCl, 1.2 mM $MgSO_4$, 2 mM $CaCl_2$, 1.2 mM KH_2PO_4, 6 mM glucose and 25 mM HEPES-Na, pH 7.4) and then incubated for 0, 5, 10, 20, 40 and 60 min with each toxin (Ntx, β-Btx, Tpx and Tetx) at 6 nM concentration in 1 mL Krebs-Ringer buffer. When needed, a 20 min pre-incubation with 1 μM ionomycin was performed. In some cases, cells were pre-treated with 50 μM aristolochic acid (AA) for 30 min before 60-min incubation with the toxins. All treatments were performed at 37°C. After intoxication, cells were broken in cold methanol, collected and pellets were frozen and kept at −20°C until analysis. Total lipids were extracted from cell pellets using $CHCl_3$–CH_3OH (2 : 1) after addition of the internal standards dimyristoylPC (2 nmol), dimyristoylphosphatidylethanolamine (0.8 nmol), dimyristoylPS (0.4 nmol), dimyristoylphosphatidic acid (0.2 nmol), dimyristoylphosphoglycerol (0.4 nmol) and heptadecanoyl LysoPC (0.4 nmol). The chloroform fraction was dried under a gentle nitrogen stream and stored at −80°C until analysis. ESI-MS was performed on a Micromass Quatro Ultima triple quadrupole mass spectrometer (Micromass, Wythenshaw, UK) equipped with an ESI interface. Dried lipid extracts were dissolved in CH_3OH : $CHCl_3$: H_2O : NH_3 (7 : 2 : 0.8 : 0.2, v : v) and injected into the mass spectrometer at a flow rate of 5 μL/min. Phosphatidylcholine (PC) and PE species

were preferentially detected using positive ionization while PS was quantified under negative ionization conditions. Following fragmentation with argon gas, PC and LysoPC molecules were quantified from precursor scans of *m/z* 184, PE and lysophosphatidylethanolamine (LysoPE) molecules by neutral loss scans of *m/z* 141 and PS and Lyso PS molecules by neutral loss scans of *m/z* 87. Data were acquired and processed using MassLynx NT software (Micromass, Wynthenshow, UK). After conversion to centroid format according to area, correction for ^{13}C isotope effects and for reduced response where appropriate of tandem MS/MS scans with increasing *m/z* values, the phospholipid species were expressed as percentages of their respective totals present in the sample.

Results

CGNs phosphatidylcholine hydrolysis by SPANs

Figure 1 shows the time–courses of LysoPC production by the four SPANs included in this study; toxin concentrations and time periods of analysis were chosen based on both the morphological and functional observations described above. Ntx displayed the fastest PLA_2 activity, closely followed by β-Btx; Tetx appeared to be a less potent PLA_2 whereas Tpx displayed an intermediate activity. While the PLA_2 activity of Ntx and β-Btx reached a plateau after 30–40 min from addition, the two multisubunit SPANs, Tpx and Tetx, were still active after 60 min and even after a longer incubation (2 h, results not shown). The present analysis was limited to 1 h because all these neurotoxins had paralysed the NMJ and bulged neurons in culture within this time limit (see Table 1).

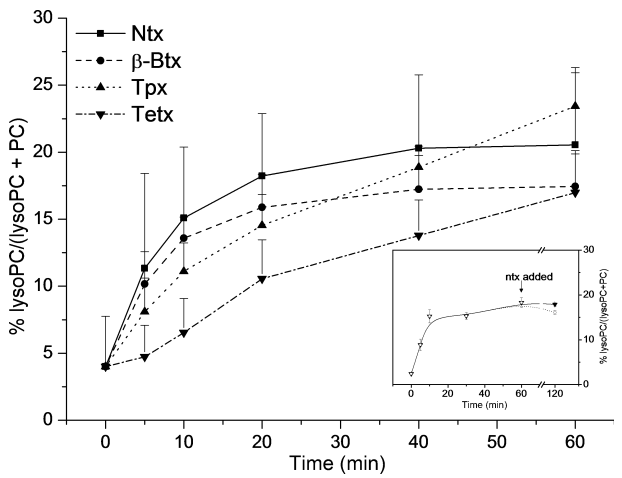

Fig. 1 Time course of Lysophosphatidylcholine (LysoPC) production by the four snake pre-synaptic PLA_2 neurotoxins. CGNs were incubated with Ntx, β-Btx, Tpx and Tetx (6 nM final concentration) for up to 1 h; PC hydrolysis was monitored and the percentage of LysoPC/LysoPC + PC plotted as a function of time. The inset shows that upon addition of fresh Ntx at 60 min (arrow, filled triangles), no further PC was hydrolysed. The determination of the time–course of the activity of each neurotoxin was performed three times in duplicates and bars are SD.

Table 1 Comparison between the time course of LysoPC production and paralysis of the mouse NMJ by the four different SPANs

	LysoPCs/ LysoPCs + PC		NMJ paralysis[a]	
	$t_{50\%}$	$t_{90\%}$	$t_{50\%}$	$t_{90\%}$
Ntx	6	27	28	50
β-Btx	6	25	22	32
Tpx	18	51	18	25
Tetx	22	52	55	74

LysoPC, lysophosphatidylcholine; NMJ, neuromuscular junction; SPANs, snake pre-synaptic PLA_2 neurotoxins; Ntx, notexin; Tpx, taipoxin; Tetx, textilotoxin; β-Btx, β-bungarotoxin.

Times at which 50% and 90% of lysoPC production (with respect to the amount obtained after 1 h of neurons exposure to the indicated neurotoxin) and of NMJ transmission blockade were determined and are reported in minutes from intoxication.

[a]Toxin concentration in mouse NMJ paralysis experiments was 1 μg/mL for Ntx, Tpx and Tetx, 3 μg/mL for β-Btx.

To ascertain whether the plateau reached by Ntx was because of its inactivation or inhibition, an equal amount of fresh toxin was added after 60 min from the first addition (see inset in Fig. 1), but no further production of LysoPC was observed. The PLA_2 activity of Ntx appears therefore to be inhibited, although we do not know if this is because of inhibition by the hydrolysis products, or lower accessibility of the phospholipid substrates or other reasons.

The amount of lipids released after 1 h of intoxication was similar in the four cases with about 17% of total cellular PC hydrolysed by Ntx, 19% by Tpx and 13% by β-Btx and Tetx. Clearly, this was a sizeable proportion of the total cell lipids. MS characterization of phospholipids composition of cerebellar neurons gave the following result: PC (59% of total phospholipids), PE (25%) and PS (15%). The time–course of LysoPC production was comparable with that of the paralysis induced by the same neurotoxins in the mouse hemidiaphragm, as shown by the comparison of their $t_{50\%}$ and $t_{90\%}$ reported in Table 1. In all cases but one, the time–course of phospholipid hydrolysis was lower than the corresponding one for NMJ paralysis and this might be taken as an additional evidence in favour of a consequentiality between PLA2 activity and blockade of the nerve terminal by these snake neurotoxins.

SPAN hydrolysis of phosphatidylethanolamine and phosphatidylserine in CGN neurons

Figure 2a shows that LysoPE was also produced by the four SPANs with time–courses comparable with that of LysoPC, but to lower extents. There was a difference among the four SPANs, with Ntx showing a much higher activity toward PE than the other three neurotoxins. In any case, the ratio LysoPC/LysoPE calculated after 1 h from toxin addition was

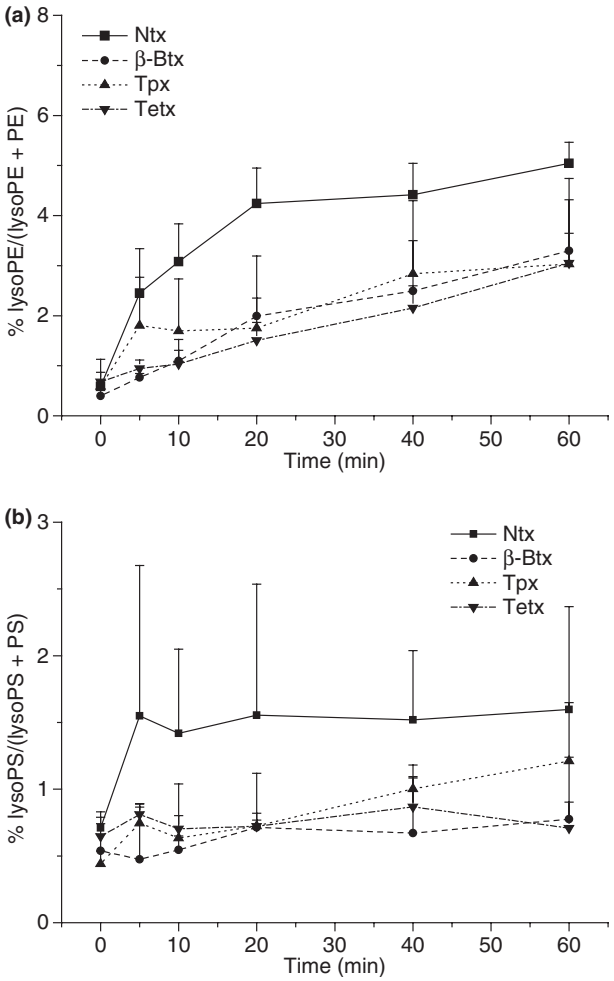

Fig. 2 Time–course of Lysophosphatidylethanolamine (LysoPE) and Lysophosphatidylserine (LysoPS) production by the four snake presynaptic PLA_2 neurotoxins. PE and PS hydrolysis by Ntx, β-Btx, Tpx and Tetx (6 nM final concentration for up to 1 h) were monitored as a function of time and expressed as percentage of LysoPE/LysoPE + PE or LysoPS/LysoPS + PS (panels A and B respectively). The determination of the time–course of the activity of each neurotoxin was performed three times in duplicates and bars are SD.

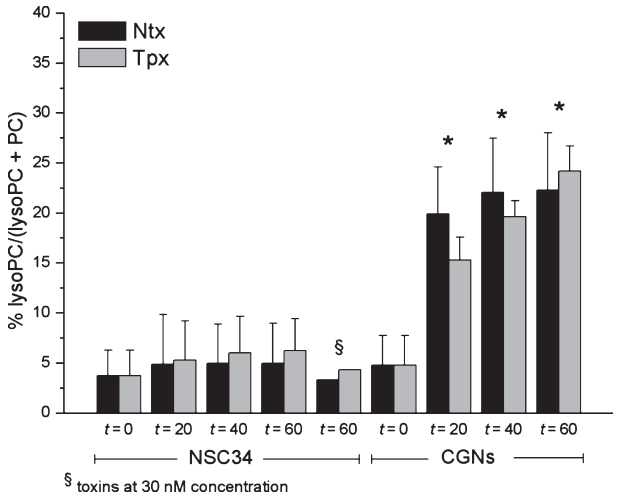

Fig. 3 Comparison between the release of LysoPC induced by Ntx and Tpx in a neuroblastoma cell line and in a primary culture of cerebellar granule neurons. Differentiated NSC34 and cerebellar granule neurons were incubated with Ntx or Tpx (6 nM) up to 1 h and the PC hydrolysis was monitored with time. Very little LysoPC was detected in intoxicated NSC34, even at higher toxin concentration (§, 30 nM), compared with the levels obtained in cerebellar neurons, suggesting that SPANs enzymatic activity is dependent on specific binding. Each bar is the result of two experiments performed in duplicates and bars represent the SD values. The data were analysed with the Student's *t*-test,* $p < 0.05$ compared to $t = 0$.

always higher than the 8 : 1 value obtained with Ntx. As the majority of PC and a minority of PE is on the outer layer of the plasma membrane (Verkleij *et al.* 1973; Fontaine *et al.* 1979; Shina *et al.* 1993), such high ratios strongly suggest that the main site of action of these neurotoxins is the outer layer of the plasma membrane. Further evidence in favour of a cell surface hydrolytic action of the SPANs is provided by the results of Fig. 2b, which shows no significant hydrolysis of PS with any of the neurotoxins in CGNs. As almost all PS is confined inside cells, and snake PLA_2s readily hydrolyse PS (Verkelij *et al.* 1973; Napias and Heilbronn 1980; Rosenberg 1997), this finding is in keeping with the above conclusion. The present results do not conflict with previous observations that SPANs enter inside neurons (Pražnikar *et al.* 2008; Rigoni *et al.* 2008), but they indicate that the internalized toxins are not very active in phospholipid hydrolysis. However, if their hydrolytic activity is concentrated on defined organelles, even minor local phospholipid hydrolysis may be sufficient to alter dramatically the organelle physiology. This consideration would be particularly relevant for mitochondria, which does interact with SPANs and are affected in their membrane permeability properties (Scorrano *et al.* 2001; Rigoni *et al.* 2007).

Limited SPAN hydrolysis of a neuroblastoma cell line

Given the limitation on isolation of pure neuronal cultures outlined in the introduction, we investigated whether transformed neuronal cultures could be used as model systems to probe the lipolytic actions of SPANs. In this respect, we evaluated the actions of SPANs on the NSC34 cell line which was developed by fusing a neuroblastoma with motor neuron-enriched embryonic spinal cord cells and was reported to preserve some characters of motoneurons, the main targets of the SPANs *in vivo* (Cashman *et al.* 1992). NSC34 cells differentiated with retinoic acid and exhibited neuronal projections and intercellular contacts. This cell line has been previously used in studies of the biological activity of snake neurotoxins (Petrovic *et al.* 2004; Pražnikar *et al.* 2008; Caccin *et al.* 2009).

Figure 3 shows that Ntx and Tpx caused the release of much lower amounts of LysoPC from differentiated NSC34

cells when compared with CGNs; their activities levelled off after 20 min with a maximum hydrolysis of only 2.5% of the cellular PC content; no increased hydrolysis was found using a high toxin concentration (30 nM). Neuronal bulging is a very sensitive morphological parameter of the *in vitro* action of SPANs (Rigoni *et al.* 2004). No bulges were observed after 20 min incubation of differentiated NSC34 incubated with 6 nM Ntx or Tpx, with only a few beginning to appear after 1 h. Taken together, these findings indicate that this neuronal cell line is not a sensitive model to study these neurotoxins. This is presumably because of defective SPAN binding, which is clearly preliminary to hydrolysis. This was demonstrated by incubation of NSC34 cells with the lysoPC + oleci acid mixture, lipids which are released by the PLA2 activity. Athought these cells have a minimal response to incubation with SPANs, these lipid mixture readily causes bulging of nerve terminals identical to that induced by SPANs in primary neurons (Caccin *et al*. 2009).

Role of calcium-activated cellular PLA2 in the phospholipid hydrolysis of CGNs

A major consequence of SPANs action on neurons is the entry of calcium from the external medium caused by the LysoPL + FA-induced increase in the ion permeability of the plasma membrane (Rigoni *et al.* 2007). The increased intracellular calcium levels could activate a series of cellular PLA_2 that could exert their enzymatic action on internal phospholipids (Orrenius *et al.* 2003). To test the possibility that at least part of the SPAN-induced phospholipids hydrolysis was because of intracellular PLA_2s, we treated CGNs with ionomycin, a well known Ca^{2+} ionophore. A minimal effect was observed (about 2% of LysoPLs production, data significance estimated with the Student's *t*-test, $p < 0.05$) (Fig. 4). Following pre-incubation with the generic cellular PLA_2 inhibitor AA (Vishwanath *et al.* 1988; Rosenthal *et al.* 1989; Chandra *et al.* 2002), no reduction in the LysoPLs production by Tetx was detected, whereas a small decrease (significative with $p < 0.05$) was observed in the case of Ntx. This latter observation might be because of the slight inhibition of the Ntx enzymatic activity itself by AA as detected by performing an *in vitro* PLA_2 assay (not shown). These findings do not exclude the possibility that PLA_2s specific for phospholipids containing in their *sn*-2 position, a particular FA, such as arachidonic acid or docosohexanoic acid, are activated to produce lipid mediators of inflammation (Piomelli *et al.* 2007), given that the proportion of these phospholipids with respect to the total amount is very low, and so escape detection.

PLA_2 activities of snake pre-synaptic neurotoxins in cultured neurons versus chemical substrates

The PLA_2 activity of snake pre-synaptic neurotoxins was always measured *in vitro* with synthetic substrates which were phospholipids of different chemical nature, usually

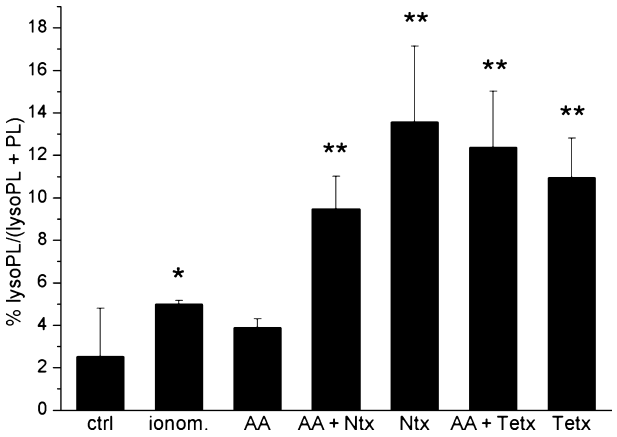

Fig. 4 Contribution of endogenous Ca^{2+}-activated PLA_2s to the lysophospholipids production measured in cerebellar granule neurons. Endogenous Ca^{2+}-activated PLA_2s were stimulated by the addition of the calcium ionophore ionomycin (1 μM) to the cultured neurons. This led to a small LysoPLs increase with respect to the control. Some samples were pre-incubated with the generic cellular PLA_2 inhibitor AA (50 μM) and exposed to Tetx or Ntx (6 nM final concentration). This did not affect LysoPLs production of Tetx and only slightly decreased Ntx LysoPLs production. Each bar is the result of four different experiments and bars are SD. The data were analysed with the Student's *t*-test,*$p < 0.05$, **$p < 0.005$ compared with control.

inserted into liposomes or lipid micelles of different compositions (Rosenberg 1997). These variables and additional factors, including buffer composition and pH values, clearly affected the measured turn-over rates. There are no reports of PLA_2 activity of SPANs measured *in vivo* or in neurons in culture. Such measurement is presented here and the data obtained throw new light on the understanding of action of these neurotoxins. Previously, there existed a large discrepancy between mouse toxicity data (fourth column of Table 2) and their PLA_2 activities measured *in vitro* (third column). Here, we have tested the PLA_2 activities of the four neurotoxins used here with a sensitive chemical method to provide a novel and coherent estimation (second column). Indeed, the present assay shows that the highly toxic Tpx, but not Tetx, is also a high turn-over PLA_2 (second column). However, here we have additionally obtained PLA_2 activity data in cultured neurons (first column), which are more biologically relevant to the *in vivo* situation. These results (first column) lead to two striking observations: (i) the activities of all the four SPANs in live neurons were much lower than those measured *in vitro* (compare the first and second columns); (ii) the PLA_2 activities of the four neurotoxins in neurons were comparable among each other, as there was only a threefold difference among the least active toxin, Tetx, and the most active one, Ntx. Clearly, the discrepancy between mouse toxicities (last column of Table 2) and PLA_2 activities remained, but it was not so unreasonable as it appeared to be before, when the two most

Table 2 Comparison between PLA2 activity of the four SPANs on cultured neurons and synthetic substrates and relative toxicity

	In vivo PLA_2 activity (nmols of PL hydrolysed/ min/nmol of toxin)	*In vitro* PLA_2 activity (nmols of PL hydrolysed/ min/nmol of toxin)	*In vitro* PLA_2 activity[a] (nmols of PL hydrolysed/ min/nmol of toxin)	Toxicity[a] (mouse LD50, μg/kg)
Ntx	49 ± 14	5009 ± 29	19 460	45
β-Btx	41 ± 12	4578 ± 149	1281	30
Tpx	19 ± 5	4500 ± 668	18	2
Tetx	15 ± 4	700 ± 248	224	1

SPANs, snake pre-synaptic PLA_2 neurotoxins; Ntx, notexin; Tpx, taipoxin; Tetx, textilotoxin; β-Btx, β-bungarotoxin; PL, phospholipids.
The data obtained here (first and second column) are the means of at least three independent experiments ± SD.
[a]Data from Rosenberg (1997).

toxic toxins (Tpx and Tetx) had the lowest PLA_2 activities. The difference remaining after this study might well be accounted for by different pharmacokinetics properties and different binding to the pre-synaptic membrane; this latter aspect has been discussed recently in terms of the quaternary structure of Tpx and Tetx (Montecucco and Rossetto 2008).

Table 2 also shows the large difference existing between the PLA_2 activities measured *in vitro* on synthetic substrates and on neurons in culture. It is very likely that most of this difference is to be attributed to the fact that in the *in vitro* assay used here the phospholipid substrate of the enzyme is a monomer in solution, endowed with a high accessibility to the active site, whilst the enzyme in neurons acts on a substrate inserted in a membrane which has to be displaced from the lipid bilayer to reach the active site of the enzyme bound to the membrane surface, as discussed before (Reynolds *et al.* 1991). Moreover, cholesterol was shown to markedly reduce the rate of phospholipid hydrolysis (Stron and Kelly 1977; Napias and Heilbronn 1980).

Discussion

The present paper reports the first detailed analysis of the PLA_2 activity of Ntx, β-Btx, Tpx and Tetx in living neurons which is made possible by modern lipid MS. This analysis revealed novel and unexpected findings that explained apparent contradictions present in the literature. In fact, previously, there appeared to be a strong discrepancy among the PLA_2 activities measured *in vitro* with synthetic substrates and the mouse toxicities of these pre-synaptic snake neurotoxins (Rosenberg 1997; Montecucco and Rossetto 2000). This is summarized in Table 2. Tetx and Tpx were reported to have the lowest *in vitro* PLA_2 activities and yet to be the most toxic of all SPANs. Their PLA_2 activity measured here with a very sensitive *in vitro* assay provided us with higher values with respect to the previous literature, but still difficult to reconcile with their toxicities. The mass spectrometric detection of the hydrolysis of PC, PE and PS catalysed by the four neurotoxins tested here in pure cultured neurons provided PLA_2 turn-over values which were comparable among the four SPANs, and expected to be closer to those displayed at the NMJ. These values slightly underestimated PLA_2 activity as hydrolysis was only measured for the major phospholipid classes (PC, PE and PS) because other cell phospholipids were present in too low amounts to be considered. However, Tetx and Tpx had PLA_2 enzymatic activities on neurons close to those of Ntx and β-Btx, but not higher. Therefore, one must invoke more favourable pharmacokinetics and/or pre-synaptic binding activities to account for the remaining difference in toxicity. Thus, the present work largely resolved a major inconsistency of the previous knowledge on the biological properties of SPANs.

The other major result obtained here, using neurons in culture, was that there was a minimal hydrolysis of PS and that the ratio of LysoPC/LysoPE was close to the PC/PE ratio present on the outer layer of the plasma membrane rather than to that of the entire cell phospholipid composition. This indicates that the major site of phospholipid hydrolysis by all the four SPANs tested here is the pre-synaptic membrane surface. This result should be considered in conjunction with several reports that observed SPANs inside cells (Herkert *et al.* 2001; Neco *et al.* 2003; Petrovic *et al.* 2004; Pražnikar *et al.* 2008; Rigoni *et al.* 2008). The present findings indicate that the cytosolic SPAN hydrolysis contributes little, if any, to the overall phospholipid hydrolysis. However, they do not exclude the possibility that limited localized hydrolysis may be of great relevance for intoxication as there are organelles very sensitive to the effect of LysoPLs and FA, such as the mitochondria to which Ntx, β-Btx and Tpx bind (Scorrano *et al.* 2001; Rigoni *et al.* 2008).

In summary, the results presented here demonstrate the limited and the site-specific phospholipase activity of this panel of pre-synaptic neurotoxins. The discrepancy between the *in vitro* PLA_2 acitivities of the various SPANs, measured in a vesicular assay, with their activity against intact neuronal cells strongly suggests that the plasma membrane microenvironment of receptor-bound SPAN molecules imposes considerable constraints on their ability to hydrolyse PC. This result may have wide implications for other categories of PLA2 effectors acting on cell membranes.

Acknowledgements

This work was supported by grants from the Fondazione CARIPARO (Physiopathology of the Synapse), Telethon GGP06133 and Regione Veneto Programma Biotech III.

References

Aquilina J. A. (2009) The major toxin from the Australian Common Brown Snake is a hexamer with unusual gas-phase dissociation properties. *Proteins* **75**, 478–485.

Caccin P., Rigoni M., Bisceglie M., Rossetto O. and Montecucco C. (2006) Reversible skeletal neuromuscular paralysis induced by different lysophospholipids. *FEBS Lett.* **580**, 6317–6321.

Caccin P., Rossetto O. and Montecucco C. (2009) Neurotoxicity of inverted-cone shaped lipids. *Neurotoxicology* **30**, 174–181.

Cashman N. R., Durham H. D., Blusztajn J. K., Oda K., Tabira T., Shaw I. T., Dahrouge S. and Antel J. P. (1992) Neuroblastoma x spinal cord (NSC) hybrid cell lines resemble developing motor neurons. *Dev. Dyn.* **194**, 209–221.

Chandra V., Jasti J., Kaur P., Srinivasan A., Betzel C. and Singh T. P. (2002) Structural basis of phospholipase A2 inhibition for the synthesis of prostaglandins by the plant alkaloid aristolochic acid from a 1.7 A crystal structure. *Biochemistry* **41**, 10914–10919.

Chen I. L. and Lee C. Y. (1970) Ultrastructural changes in the motor nerve terminals caused by beta-bungarotoxin. *Virchows Arch. B. Cell. Pathol.* **6**, 318–325.

Connolly S., Trevett A. J., Nwokolo N. C. *et al.* (1995) Neuromuscular effects of *Papuan Taipan* snake venom. *Ann. Neurol.* **38**, 916–920.

Davis B., Koster G., Douet L. J. *et al.* (2008) Electrospray ionization mass spectrometry identifies substrates and products of lipoprotein-associated phospholipase A2 in oxidized human low density lipoprotein. *J. Biol. Chem.* **283**, 6428–6437.

Fontaine R. N., Harris R. A. and Schroeder F. (1979) Neuronal membrane lipid asymmetry. *Life Sci.* **24**, 395–399.

Gandolfo G., Lambeau G., Lazdunski M. and Gottesmann C. (1996) Effects on behaviour and EEG of single chain phtospholipases A2 from snake and bee venoms injected into rat brain: search for a functional antagonism. *Pharmacol. Toxicol.* **78**, 341–347.

Gutiérrez J. M., Theakston R. D. G. and Warrel D. A. (2006) Confronting the neglected problem of snake bite envenoming: the need for a global partnership. *PLoS Med.* **3**, 727–731.

Han X. and Gross R. W. (2003) Global analyses of cellular lipidomes directly from crude extracts of biological samples by ESI mass spectrometry: a bridge to lipidomics. *J. Lipid Res.* **44**, 1071–1079.

Harris J. B., Grubb B. D., Maltin C. A. and Dixon R. (2000) The neurotoxicity of the venom phospholipases A2, notexin and taipoxin. *Exp. Neurol.* **161**, 517–526.

Herkert M., Shakhman O., Schweins E. and Becker C. M. (2001) Beta-bungarotoxin is a potent inducer of apoptosis in cultured rat neurons by receptor-mediated internalization. *Eur. J. Neurosci.* **14**, 821–828.

Kini R. M. (2003) Excitement ahead: structure, function and mechanism of snake venom phospholipase A2 enzymes. *Toxicon* **42**, 827–840.

Kolko M., Bruhn T., Christensen T., Lazdunski M., Lambeau G., Bazan N. G. and Diemer N. H. (1999) Secretory phospholipase A2 potentiates glutamate-induced rat striatal neuronal cell death *in vivo*. *Neurosci. Lett.* **274**, 167–170.

Lasher R. S. and Zaigon I. S. (1972) The effect of potassium on neuronal differentiation in cultures of dissociated newborn rat cerebellum. *Brain Res.* **41**, 428–488.

Levi G., Aloisi F., Ciotti M. T. and Gallo V. (1984) Autoradiographic localization and depolarization-induced release of acidic amino acids in differentiating cerebellar granule cell cultures. *Brain Res.* **290**, 77–86.

Montecucco C. and Rossetto O. (2000) How do presynaptic PLA2 neurotoxins block nerve terminals? *Trends Biochem. Sci.* **25**, 266–270.

Montecucco C. and Rossetto O. (2008) On the quaternary structure of taipoxin and textilotoxin: the advantage of being multiple. *Toxicon* **51**, 1560–1562.

Napias C. and Heilbronn E. (1980) Phospholipase A2 activity and substrate specificity of snake venom presynaptic toxins. *Biochemistry* **19**, 1146–1151.

Neco P., Rossetto O., Gil A., Montecucco C. and Gutiérrez L. M. (2003) Taipoxin induces F-actin fragmentation and enhances release of catecholamines in bovine chromaffin cells. *J. Neurochem.* **83**, 329–337.

Nicholls D., Snelling R. and Dolly O. (1985) Bioenergetic actions of beta-bungarotoxin, dendrotoxin and bee-venom phospholipase A2 on guinea-pig synaptosomes. *Biochem. J.* **229**, 653–662.

Orrenius S., Zhivotovsky B. and Nicotera P. (2003) Regulation of cell death: the calcium-apoptosis link. *Nature Rev. Mol. Cell. Biol.* **4**, 552–565.

Petrovic U., Sribar J., Paris A., Rupnik M., Krzan M., Vardjan N., Gubensek F., Zorec R. and Krizaj I. (2004) Ammodytoxin, a neurotoxic secreted phospholipase A(2), can act in the cytosol of the nerve cell. *Biochem. Biophys. Res. Commun.* **324**, 981–985.

Piomelli D., Astarita G. and Rapaka R. (2007) A neuroscientist's guide to lipidomics. *Nat. Rev. Neurosci.* **8**, 743–754.

Postle A. D., Wilton D. C., Hunt A. N. and Attard G. S. (2007) Probing phospholipid dynamics by electrospray ionisation mass spectrometry. *Prog. Lipid Res.* **46**, 200–224.

Prasarnpun S., Walsh J., Awad S. S. and Harris J. B. (2005) Envenoming bites by kraits: the biological basis of treatment-resistant neuromuscular paralysis. *Brain* **128**, 2987–2996.

Pražnikar Z. J., Kovačič L., Rowan E. G., Romih R., Rumini P., Poletti A., Križaj I. and Pungerčar J. (2008) A presynaptically toxic secreted phospholipase A2 is internalized into motoneuron-like cells where it is rapidly translocated into the cytosol. *Biochim. Biophys. Acta* **1783**, 1129–1139.

Pulfer M. and Murphy R. C. (2003) Electrospray mass spectrometry of phospholipids. *Mass Spectrom. Rev.* **22**, 332–364.

Rehm H. and Betz H. (1982) Binding of beta-bungarotoxin to synaptic membrane fractions of chick brain. *J. Biol. Chem.* **257**, 10015–10022.

Reynolds L. J., Washburn W. N., Deems R. E. and Dennis E. A. (1991) Assay strategies and methods for phospholipases. *Methods Enzymol.* **197**, 3–23.

Reynolds L. J., Hughes L. L. and Dennis E. A. (1992) Analysis of human synovial fluid phospholipase A2 on short chain phosphatidylcholine-mixed micelles: development of a spectrophotometric assay suitable for a microtiterplate reader. *Anal. Biochem.* **204**, 190–197.

Rigoni M., Schiavo G., Weston A. E., Caccin P., Allegrini F., Pennuto M., Valtorta F., Montecucco C. and Rossetto O. (2004) Snake presynaptic neurotoxins with phospholipase A2 activity induce punctate swellings of neurites and exocytosis of synaptic vesicles. *J. Cell Sci.* **117**, 3561–3570.

Rigoni M., Caccin P., Gschmeissner S., Koster G., Postle A. D., Rossetto O., Schiavo G. and Montecucco C. (2005) Equivalent effects of snake PLA2 neurotoxins and lysophospholipid-fatty acid mixtures. *Science* **310**, 1678–1680.

Rigoni M., Pizzo P., Schiavo G., Weston A. E., Zatti G., Caccin P., Rossetto O., Pozzan T. and Montecucco C. (2007) Calcium influx and mitochondrial alterations at synapses exposed to snake

neurotoxins or their phospholipid hydrolysis products. *J. Biol. Chem.* **282**, 11238–11245.

Rigoni M., Paoli M., Milanesi E., Caccin P., Rasola A., Bernardi P. and Montecucco C. (2008) Snake phospholipase A2 neurotoxins enter neurons, bind specifically to mitochondria, and open their transition pores. *J. Biol. Chem.* **283**, 34013–34020.

Rosenberg P. (1997) Lethal potency of snake venom phospholipase A2 enzymes, in *Venom Phospholipase A2 Enzymes: Structure, Function and Mechanism* (Kini R. M., ed), pp. 129–154. John Wiley & Sons, Chichester.

Rosenthal M. D., Vishwanath B. S. and Franson R. C. (1989) Effects of aristolochic acid on phospholipase A2 activity and arachidonate metabolism of human neutrophils. *Biochim. Biophys. Acta* **1001**, 1–8.

Rugolo M., Dolly J. O. and Nicholls D. G. (1986) The mechanism of action of beta-bungarotoxin at the presynaptic plasma membrane. *Biochem. J.* **233**, 519–523.

Shina R., Crain R. C., Rosenberg P. and Condrea E. (1993) The asymmetric distribution of phosphatidylcholine in rat brain synaptic plasma membranes. *Neurochem. Int.* **22**, 189–195.

Scorrano L., Penzo D., Petronilli V., Pagano F. and Bernardi P. (2001) Arachidonic acid causes cell death through the mitochondrial permeability transition Implications for tumor necrosis factor-alpha aopototic signaling. *J. Biol. Chem.* **276**, 12035–12040.

Stron P. N. and Kelly R. B. (1977) Membranes undergoing phase transitions are preferentially hydrolyzed by beta-bungarotoxin. *Biochim. Biophys. Acta* **469**, 231–235.

Verkleij A. J., Zwaal R. F., Roelofsen B., Comfurius P., Kastelijn D. and van Deenen L. L. (1973) The asymmetric distribution of phospholipids in the human red cell membrane. A combined study using phospholipases and freeze-etch electron microscopy. *Biochem. Biophys. Acta.* **323**, 178–193.

Vishwanath B. S., Fawzy A. A. and Franson R. C. (1988) Edema-inducing activity of phospholipase A2 purified from human synovial fluid and inhibition by aristolochic acid. *Inflammation* **12**, 549–561.

Wilensky R. L., Shi Y., Mohler E. R. III *et al.* (2008) Inhibition of lipoprotein-associated phospholipase A2 reduces complex coronary atherosclerotic plaque development. *Nat. Med.* **14**, 1059–1066.

4

PRELIMINARY ANALYSIS OF AUSTRALIAN TAIPAN VENOM COMPOSITION. CHARACTERIZATION AND ISOLATION OF TAIPOXIN SUBUNITS FOR STRUCTURAL ANALYSIS.*

*This work has been done in collaboration with Dr. Laura Cendron, Dr. Patrizia Polverino, and Prof. Giuseppe Zanotti

1.1 Introduction

With a mouse LD_{50} of 12 μg/kg, the venom of the Australian taipan *Oxyuranus scutellatus scutellatus* is one of the most poisonous of the animal kingdom (Fohlman *et al.*, 1976). Snake venoms are reportedly a mixture of various toxic component: fibrinolytic proteases (Suhr and Kim, 1996), prothrombin activators (Speijer *et al.*, 1986), secretory phospholipase A_2 (Kini, 1997), L-amino acid oxydase (Du and Clemetson, 2002), and metalloproteinases (Gomis-Ruth *et al.*, 1993), plus other toxic and non toxic peptides. Although different components concur to the toxicity of the venom, the main effect encountered in envenomated subjects is the rapid neuromuscular junction paralysis. The major responsible for the neurotransmission blockade is taipoxin, a multichain presynaptic PLA_2 neurotoxin (Fohlman *et al.*, 1976; Harris and Maltin, 1982). Taipoxin, one of the most lethal toxins produced by animals, is endowed with a very high specificity for the presynaptic nerve terminal, where it is able to concentrate its catalytic activity, thus reaching a mouse LD_{50} of 2 μg/kg.

Oxyuranus s. scutellatus venom can be separated in gel filtration chromatography into three main protein fractions: a high molecular weight (>100 kDa), a medium molecular weight (about 45 kDa), and a low molecular weight fraction (<20 kDa) (Fohlman *et al.*, 1976). The main component of the high molecular weight pool is reportedly a prothrombin activator, a high molecular weight multimeric complex, involved not in neurotoxicity but in blood coagulation (Walker *et al.*, 1980; Speijer *et al.*, 1986). The intermediate fraction has already been intensively analyzed in the past decades due to its high neurotoxic effect and it has been identified as taipoxin, a trimeric phospholipase A_2 neurotoxin (Fohlman *et al.*, 1976). Taipoxin structural complexity and composition were hence investigated by dissociation experiments and subunit alpha, beta, and gamma were identified as the basic units of the heterotrimer. The third fraction represents the major protein fraction of the SEC separated venom but, nonetheless, the least characterized.

In this study, mass spectrometry analysis of fraction II components was performed, in order to finely characterize taipoxin subunit composition, and to purify them for successive structural analysis. Surprisingly, gamma subunit could not be detected in the dissociated taipoxin, hence a systematic mass spectrometry analysis of the low molecular weight fraction III was carried on to test the possibility to find in this low molecular weight protein pool the

dissociated gamma subunit. This study has been preliminary to structural analysis *via* X-ray crystallography of taipoxin subunits.

1.2 Material and methods

Venom

Dried *Oxyranus s. scutellatus* venom was purchased by Venom Supplies, Tanunda, South Australia. The analyzed batch was obtained from pooling the venom of seven individual snakes.

Size exclusion chromatography

Crude venom was dissolved at the desired concentration (up to 0.06 mg/mL) in 0.1 M ammonium acetate, pH 6.5; insoluble material was removed by centrifugation 5 minutes at 16,000 g. The homogeneous solution was applied to a Superdex 200 10/300 chromatographic column equilibrated with 0.1 M ammonium acetate, pH 6.5. The collected protein fractions were either employed within a few hours for toxicity screening or in SDS-PAGE or lyophilized and stored at -20°C.

Reverse phase-high performance liquid chromatography

Size exclusion purified fractions II and III were denatured in 8 M guanidine chloride for 1 hour and separated in reverse phase high pressure liquid chromatography. Fraction II was separated *via* a 5 µm C18 300 Å, 150 x 4.60 mm Phenomenex Jupiter equilibrated in TFA 0.085% in H_2O. The elution occurred in TFA 0.085% in acetonitrile in an optimized gradient (35-45% solvent B in 40 min, 45-95% solvent B in 20 min). Fraction III was separated *via* a 5 µm C18 300 Å, 250 x 10.00 mm Phenomenex Jupiter equilibrated in TFA 0.085% in H_2O. In this case, elution occurred in a continuous gradient (5-95% in 55 min) of TFA 0.085% in acetonitrile.

Cell culture

Rat cerebellar granule neurons (CGNs) were prepared from 6-days-old Wistar rats as previously described (Levi et al. 1984) and plated at 2 x 106 cells per 35 mm Petri dish. Cells were used 6 days after plating.

Mass spectrometry analysis and N-terminal sequencing

For electrospray ionization mass spectrometry (ESI-MS) analysis, the fractionated venom was dried out and eluted in 50% acetonitrile containing 0.2% formic acid. Data were collected on a Micromass Q-Tof spectrometer (Manchester, UK) (capillary voltage: 3000–3200 V; cone voltage: 45 V; scan time: 1 s; interscan: 0.1 s). Spectra were analyzed using Micromass Mass-Lynx. N-terminal sequencing was performed from CEINGE, Biotecnologie Avanzate s.c.a r.l., Proteomics Laboratory (Rome, Italy).

1.3 Results

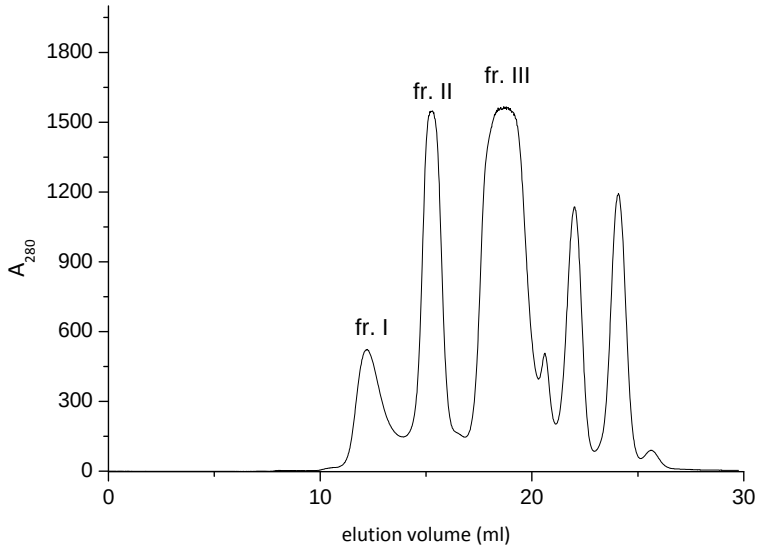

Figure 1. Gel filtration chromatography of 10 mg of *O. s. scutellatus* venom resuspended in ammonium acetate 0.1 M buffer, pH 6.5. Fractions of interest are identified as fractions I, II, and III.

Venom fractionation

Lyophilized venom of *Oxyuranus s. scutellatus* was resuspended in ammonium acetate 100 mM and separated via size exclusion chromatography (Figure 1). In concordance with previous literature (Fohlman *et al.*, 1976; Fohlman, 1978), three main fractions (I, II, and III) could be clearly separated, whereas a fourth low molecular weight fraction (fraction IV) appeared only as a minor shoulder downstream third peak. Fractions I to III were separately tested for neurotoxic activity on cerebellar granule neurons primary cultures. As shown in Figure 2, peak I induced neuronal bulging only at high concentration (>100 μg/ml), while at 1 μg/ml does not show any neurotoxic activity. On the contrary, both peaks II and III provoked neuronal damage already at 1 μg/ml concentration. Fractions II and III were the only endowed with relevant neurotoxicity and have been further analyzed for their protein composition.

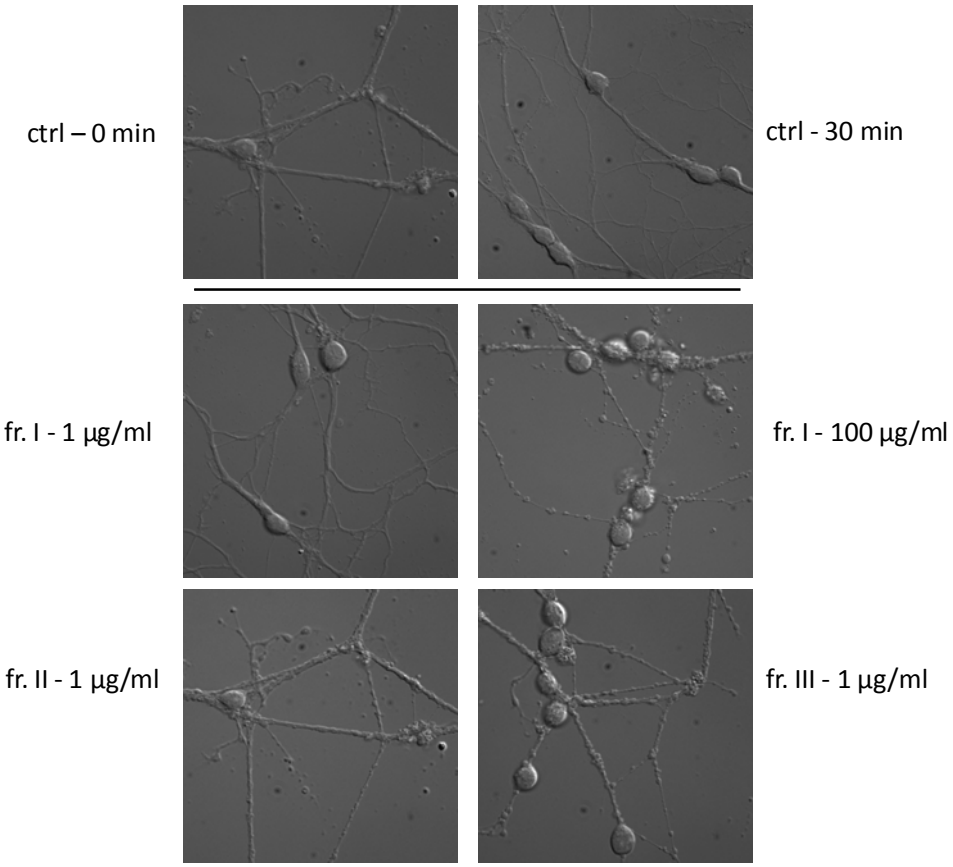

Figure 2. Cerebellar granule neurons threated with fractions I to III. Neurons were exposed to the venom fractions at the indicated concentrations for 30 minutes. The uprising of enlargements along the neuronal processes indicates presence of neurotoxic activity.

Fraction II characterization:

Fraction II accounts for almost 30% of the total protein content of the venom. Its elution volume implies an average molecular weight of the protein content of about 45 kDa. Furthermore, the elevated toxicity of the fraction suggests taipoxin, the 45 kDa multichain PLA_2 neurotoxin, as the main (possibly the sole) component of the protein pool. As described in materials and methods, the purified fraction was denatured in guanidine chloride for 1 hour to favour the separation of taipoxin into subunits, and of other possible components of the fraction. The dissociated fraction was further separated in reverse phase chromatography revealing a fairly simple elution profile with seven major peaks (named from A to G) concentrated in a very restricted zone of the acetonitrile gradient (Figure 3). In Table 1 is reported the composition of the peaks in molecular masses (MM). With the exception of peak A, showing a MM of about 6.8 kDa, all peaks report MMs of the size of the basic $sPLA_2$ unit (~13.5 kDa) of the trimeric taipoxin. Three mass species are individuated in fractions from B to E: 14 kDa (B), about 13.3 kDa (C and D), and 13.8 kDa (E). Peaks F and G, more heterogeneous, appear as mixtures of the same masses detected in peaks B to E.

Table 1. Fraction II components were separated in reverse phase chromatography and analyzed in ESI-MS. When performed, N-terminal sequence and presence of neurotoxic activity tested on CGNs is reported.

reverse phase purified fractions	mass spectrometry (Da)	elution time (min)	N-terminal sequencing	Neurotoxicity
A	6786.86±0.04 6802.29±0.47 6767.98±0.05	47.0	**---**	---
B	13987.85±0.84	50.5	Asn-Leu-Leu-Gln (*alpha*)	Yes
C	13307.27±0.08 13236.29±0.14	56.0	Asn-Leu-Val-Gln (*beta*)	No
D	13307.27±0.08 13236.29±0.14	57.8	Asn-Leu-Val-Gln (*beta*)	No
E	13812.40±0.26	61.5	**---**	Yes
F	13334.39±0.69 13813.44±0.45	72.0	**---**	**---**
G	13814.65±0.88 13928,41±0.12 13334.78±0.87	74.1	**---**	**---**

Pure fractions (B-E) were tested for neurotoxic activity on cerebellar granule neurons (Figure 4). Cell cultures were intoxicated with 10 nM concentration of each isolated protein pool. Fractions B and E induced bulges formation along the processes of intoxicated neurons, whereas no neurotoxicity was detected after incubation with fractions C or D in the same conditions. A comparison with the expected masses of taipoxin subunits was performed. In particular, peak E was observed to match almost perfectly the expected MM of alpha subunit (13812 Da experimental and 13813 Da expected); peaks C and D showed masses in the proximity of beta subunit expected molecular weight (13.236 Da); peak B MM appeared greater than the predicted weight of the alpha subunit, but it was also too little to refer to gamma subunit (prediction based on gamma subunit amino acid sequence provides a MM of 14.6 kDa, but its mass is reportedly 18.5 kDa due to presence of carbohydrates residues). N-terminal sequencing on the still uncertain protein fractions B to D was performed. The outcome (reported in Table 1) revealed unequivocally the nature of the fractions components. In concordance with the reported neurotoxic activity and also with the little difference observed between measured and expected MM, fractions B appeared to be composed by alpha subunits PLA_2, whereas isoforms of beta subunit constitute peaks C and D. On our way towards the definition of taipoxin subunit composition and towards the isolation of the subunits for structural characterization of the monomers and of the trimeric toxin, it was quite surprising not being able to detect the gamma subunit among the major fractions of dissociated functional taipoxin. Because of the possibility that gamma subunit could be not necessarily part of the toxin but just an independent monomeric $sPLA_2$, and to extend our knowledge of the venom composition to the major protein fraction III, a systematic mass spectrometry analysis of the low molecular weight pool was performed.

Fraction III characterization

Fraction III represents the main protein fraction of the Australian taipan venom (51±5%), and its elution profile suggests an average size of the peak components of about 15 kDa. Following denaturation its content was separated in reverse phase chromatography, as described in materials and methods. With respect to fraction II, fraction III is more dispersed along the acetonitrile gradient, suggesting a more heterogeneous composition concerning the hydrophobicity of

the proteins (Figure 5). In Table 2 are reported the molecular masses detected in the more significant protein peaks. In this fraction, three very different protein pools were detected. The first peaks to be eluted in the acetonitrile gradient show a MM of about 7 kDa, the second group of masses (the more consistent) are attested at about 13.5 kDa, whereas only one last peak shows a weight of 24 kDa. Clearly, the middle fraction has a high correspondence with the components detected in fraction II, described in the previous paragraph.

Table 2. Fraction III components were separated in reverse phase chromatography and analyzed in ESI-MS.

Reverse phase purified fractions	Mass spectrometry (Da)
a	6786.86±0.04
b	6802.66±0.40
c	7222.98±0.26
d	7264.17±0.03
e	13401.32±0.29
f	13317.34±0.08 13222.15±0.02 13410.40±0.12
g	13550.48±0.05 13648.96±0.11
h	14086.18±0.11 13303.55±0.37
i	13232.95±0.03 14086.50±0.02 13262.88±0.04 13303.39±0.06
j	13334.89±0.09 14059.46±0.05
k	24297.71±0.16 24396.37±0.55

In particular, the detected masses are generally concentrated around 13.9 kDa and 13.3 kDa, similarly to the masses detected in the previous analyzed fraction. Possibly, those molecular weights belong to $sPLA_2$ subunits which were either dissociated from the trimeric taipoxin before the first size exclusion separation of the venom, or they were actually present in the venom in the monomeric form. In any case, a dynamic equilibrium between the trimeric and the monomeric

aggregation state can be excluded. In fact, upon re-elution in size exclusion chromatography of purified taipoxin, only a single peak at the elution volume of the trimeric complex was detected, and no 14 kDa peak was observed (data not shown). No components of molecular mass attributable to taipoxin gamma subunit was detected.

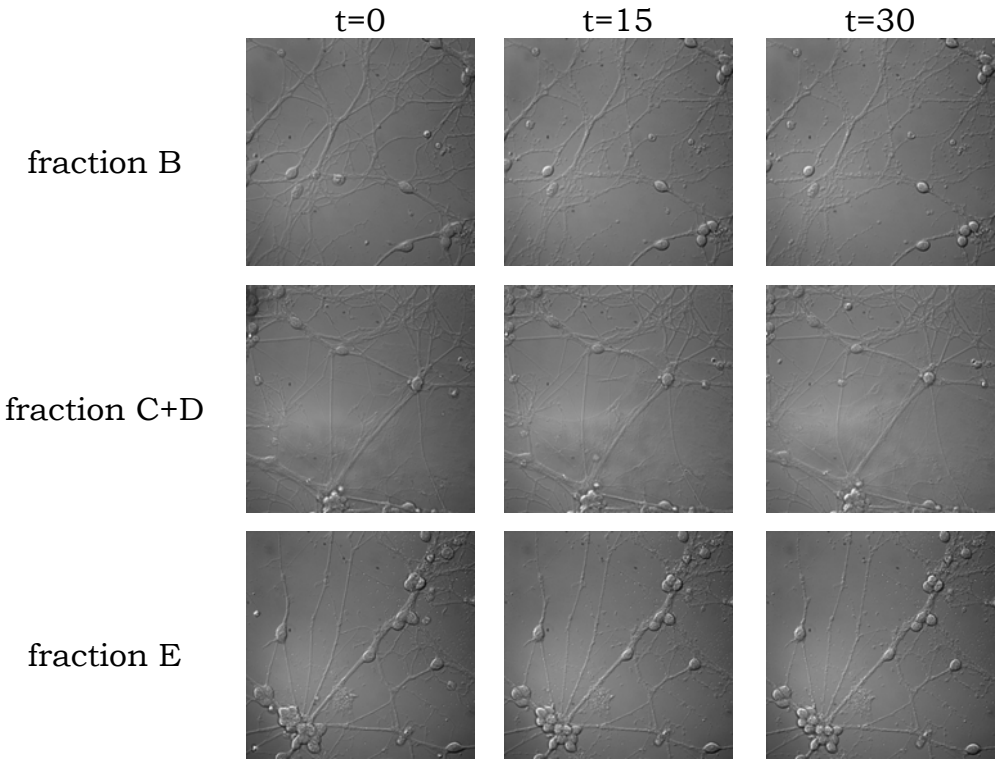

Figure 3. Cerebellar granule neurons were exposed to 10 nM concentration of peaks B to E. Genesis of bulges along the neuronal processes indicates the presence of neurotoxic activity.

1.4 Discussion

Of three subpopulations isolated in gel filtration chromatography from *O. s. scutellatus* venom, two are endowed with neurotoxic activity. Fraction II was clearly constituted by taipoxin. This conclusion was suggested by elution volume and by the pronounced neurotoxic activity. Fully functional taipoxin was then exposed to denaturing agents to dissociate it and characterize its subunit composition. Fractionation in reverse phase chromatography revealed peaks of different homogeneity in molecular mass. Among all, four peaks resulted pure in

composition and two masses with similar values to predicted taipoxin subunits molecular weights were identified. Peaks B and E showed molecular masses of about 13.9 kDa, similar to alpha subunit molecular mass. Further analysis on their toxicity at low concentration on neuronal primary cultures, and N-terminal sequencing of peak B content, confirm the association of the peaks in questions with subunit alpha. Moreover, this indicates that the subunit is still functional after denaturation and exposure to acetonitrile. Peaks C and D, instead, were identified from their molecular mass, their lack of neurotoxic activity, and their N-terminal sequence, as composed by taipoxin beta subunit. While subunits alpha and beta were observed (as expected), subunit gamma was not found in our investigations, suggesting the possibility of a functional taipoxin in absence of gamma subunit. Another major fraction of the venom, fraction III, was tested positive to neurotoxicity assay and therefore analyzed in its components. Three protein components were revealed: several fractions of PLA_2-like proteins of a molecular mass of about 13.5 kDa; a fraction of higher molecular weight proteins (about 24 kDa); and four minor fractions of molecular masses of 7 kDa. However, no trace of gamma subunit molecular mass was detected in fraction III. This rules out the possibility that gamma subunit was not detected among taipoxin subunits because present in the venom just as a monomeric $sPLA_2$. Further purification trials on different venom batches and with different chromatographic methods will be employed in the attempt to isolate gamma subunit. Further analysis need to be performed before drawing any conclusion relative to the nature of fraction III neurotoxicity. However, the massive presence of compounds whose masses remind of taipoxin alpha subunit, suggests that fraction III hosts neurotoxic monomeric $sPLA_2$.

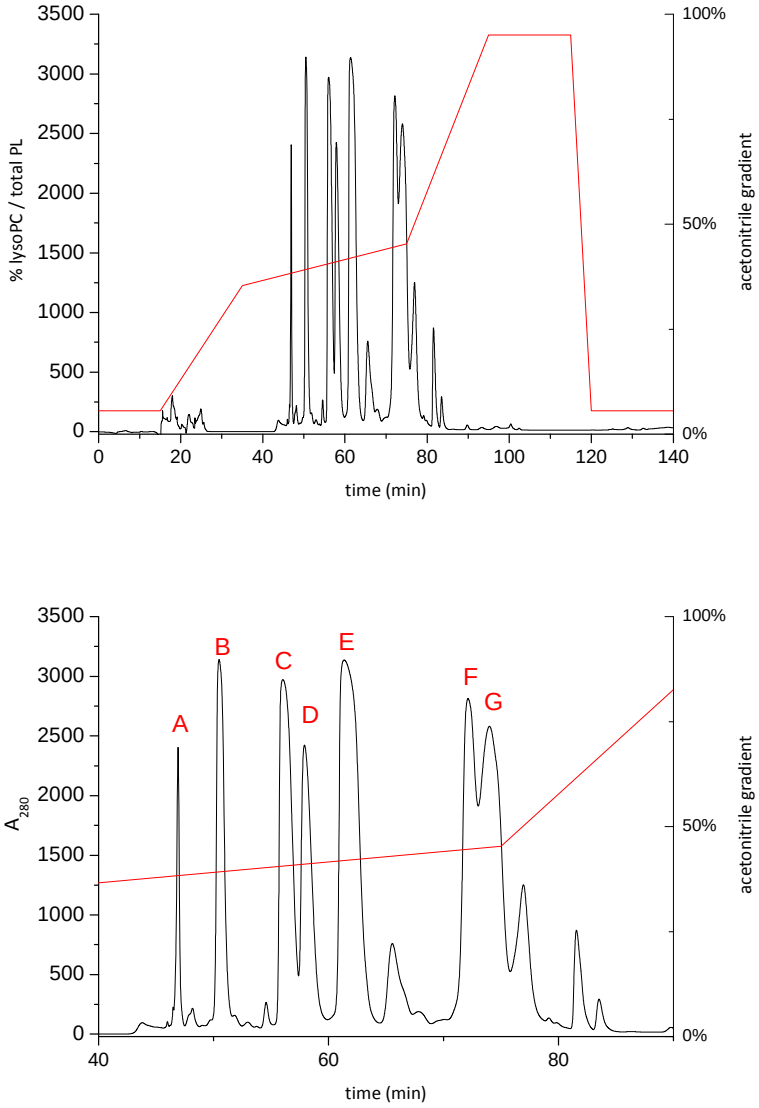

Figure 4. Reverse phase chromatography elution profile of denatured fraction II (top).. At the bottom is reported a zoom on the region of interest and analyzed fractions are identified with letters from **A** to **G**.

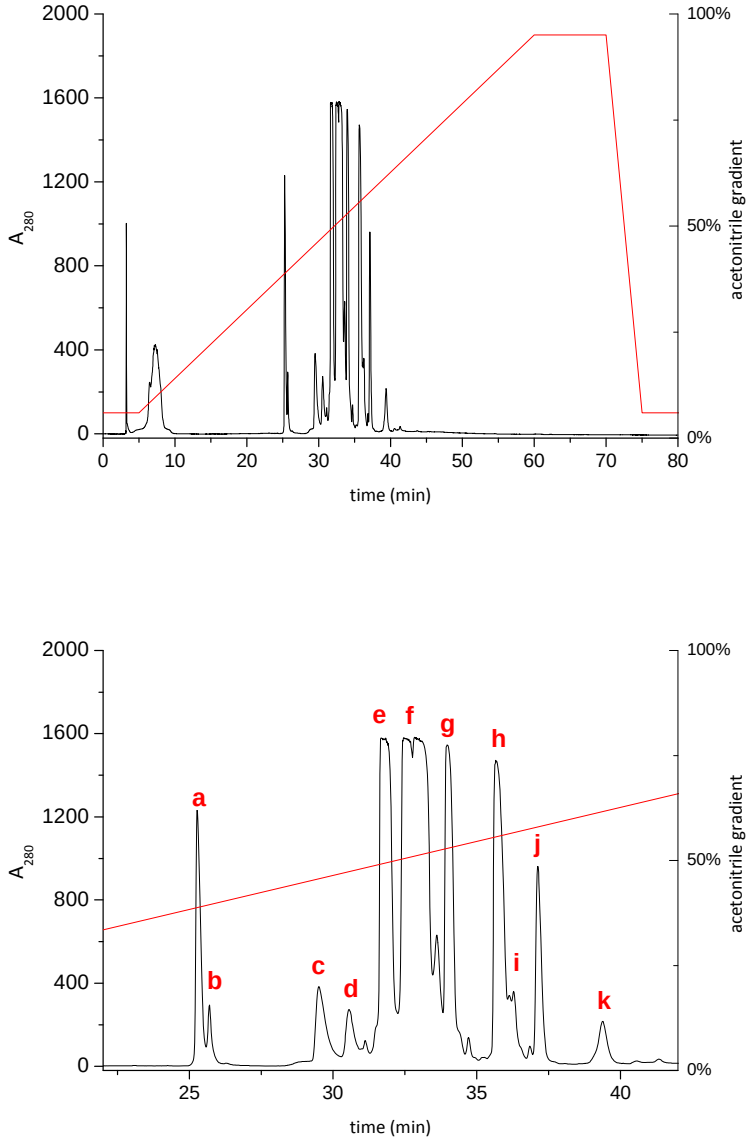

Figure 5. Reverse phase chromatography elution profile of denaturated fraction III (top). At the bottom is shown a zoom on the region of interest and analyzed fractions are identified with letters from **a** to **k**.

References

Du XY, Clemetson KJ (2002) Snake venom L-amino acid oxidases. *Toxicon* 40(6):659-65

Fohlman J, Eaker D, Karlsoon E, Thesleff S (1976) Taipoxin, an extremely potent presynaptic neurotoxin from the venom of the australian snake taipan (*Oxyuranus s. scutellatus*). Isolation, characterization, quaternary structure and pharmacological properties. *Eur J Biochem* 68(2):457-69

Gomis-Rüth FX, Kress LF, Bode W (1993) First structure of a snake venom metalloproteinase: a prototype for matrix metalloproteinases/collagenases. *EMBO J* 12(11):4151-7

Harris JB, Maltin CA (1982) Myotoxic activity of the crude venom and the principal neurotoxin, taipoxin, of the Australian taipan, *Oxyuranus scutellatus*. *Br J Pharmacol* 76(1):61-75

Kini RM (1997) Venom phospholipase A2 enzymes. John Wiley & Sons, Chichester

Speijer H, Govers-Riemslag JW, Zwaal RF, Rosing J (1986) Prothrombin activation by an activator from the venom of *Oxyuranus scutellatus* (Taipan snake). *J Biol Chem* 261(28):13258-67

Suhr SM, Kim DS (1996) Identification of the snake venom substance that induces apoptosis. *Biochem Biophys Res Commun* 224(1):134-9

Walker FJ, Owen WG, Esmon CT (1980) Characterization of the prothrombin activator from the venom of *Oxyuranus scutellatus scutellatus* (taipan venom). *Biochemistry* 19(5):1020-3

5

PRELIMINARY STUDIES OF TAIPOXIN QUATERNARY ORGANIZATION. STRUCTURAL ANALYSIS OF TAIPOXIN BETA SUBUNIT.*

*This work has been done in collaboration with Dr. Laura Cendron and Prof. Giuseppe Zanotti

1.5 Introduction

Taipoxin is a major component of the venom of the Australian taipan snake *Oxyuranus scutellatus scutellatus* (Fohlman *et al.*, 1976). It specifically binds to the presynaptic nerve terminal and hydrolyzes the plasma membrane phospholipids into lysophospholipids and fatty acids. The disruption of the nerve terminal plasma membrane triggers an unbalanced synaptic vesicle exocytosis, and in consequence a rapid paralysis of the neuromuscular junction (Montecucco *et al.*, 2008). Taipoxin is a multichain phospholipase A_2 (PLA_2) neurotoxin, composed by three homologous secretory PLA_2 non covalently bound. The three subunits, namely alpha, beta, and gamma, are reportedly in a 1 : 1 : 1 ratio in the toxin (Fohlman *et al.*, 1976). All three subunits belong to class I secretory PLA_2, a group of relatively small (molecular weight of about 14 kDa) and fairly homologous Ca^{2+}-dependent enzymes, which fold into three α-helices, a backbone loop and an antiparallel β-strand. Seven intrachain disulfide bridges cross-link the monomers conferring them a high resistance to denaturation. Alpha subunit, 119 amino acids and predicted molecular mass of 13.8 kDa, is the sole subunit for which the phospholipase A_2 activity appears to be fully conserved (Fohlman *et al.*, 1979; Lind and Eaker, 1982). Beta subunit, 118 amino acids and a predicted mass of 13.2 kDa, is a neutral protein that can be distinguished in ionic exchange chromatography in two isoforms, beta-1 and beta-2, with a slightly different amino acid composition (Fohlman *et al.*, 1976). Both isosubunits seem to have almost completely lost their enzymatic activity, probably due to a partial inability to bind the Ca^{2+} necessary for the catalytic reaction (Fohlman *et al.*, 1979). Gamma subunit is larger (133 amino acids, MW=18.5 kDa) and it conserves very little enzymatic activity (Fohlman *et al.*, 1976; 1977; 1979). Moreover, its experimental molecular weight is significantly higher than the predicted one. In fact, gamma subunit experimental weight is reportedly about 18.5 kDa, and the difference from the predicted 14.6 kDa is due to a large presence of carbohydrates on the subunit surface (Fohlman *et al.*, 1976). Fohlman and colleagues (1979) performed a complete analysis of the catalytic activity and neurotoxicity of taipoxin and of its three subunits. The *in vitro* activity, measured as μmols of hydrolyzed phospholipids per minute per mg of toxin (or subunit), revealed an activity of 0.4 for the whole toxin and respectively of 3.8, 0.00, and 0.7 for the subunits alpha, beta, and gamma. The alpha subunit is endowed with the highest catalytic activity, and also neurotoxicity was found to be prevalent on subunit alpha (mouse LD_{50} = 0.3 mg/kg) with respect to subunits beta and

gamma (mouse LD_{50}>2.0 mg/kg). However, whole toxin PLA_2 activity is significantly lower than the sum of the reported activity of the single subunits, whereas neurotoxicity is several times greater in the trimeric complex (mouse LD_{50}=0.002 mg/kg) than in the single subunits (Fohlman *et al.*, 1979). The aggregation of secretory PLA_2 into multimeric complexes observed in taipoxin is a recurrent evolutive behavior reported also for other snake PLA_2 neurotoxins (i.e. textilotoxin). This process leads to a loss in total phospholipases activity of the multimeric complex with respect to the activity of the single subunits in exchange for an increase in total neurotoxicity. However, no quaternary structure beyond the dimeric aggregation state is available to allow further speculations on their molecular mechanism of binding. The lack of characterized multichain structures is possibly due to the heterogeneity of the PLA_2 subunits and to the variable subunits stoichiometry inside the complex, both features known to lower the probability of crystal formation. Towards the characterization of taipoxin quaternary structure, preliminary crystallographic trials on whole taipoxin were performed. Probably because of the above mentioned reasons, the attempts were unsuccessful. Due to the failure of whole toxin structural characterization, we decided to proceed with the crystallization and structure determination of the single subunits. We present here the crystallographic structure of beta subunit isolated from the trimeric neurotoxin.

1.6 Matherials and Methods

Venom

Dried *Oxyranus scutellatus scutellatus* venom was purchased by Venom Supplies, Tanunda, South Australia. The analyzed batch was obtained from pooling the venom of seven individual snakes.

Protein purification

Taipoxin was isolated from whole venom in gel filtration chromatography. Successively, taipoxin subunits were isolated *via* reverse phase chromatography after 1 hour denaturation in 8 M guanidine chloride. The purification methods

are described in details in the previous chapter. For crystallization trials, a total amount of about 0.2 g of lyophilized venom was employed.

Protein crystallization

Whole taipoxin crystallization trials were performed with SS-I and SS-II (Structure Screen I and II, Molecular Dimension ltd), PACT and PEG'S-II (Qiagen); beta subunit trials were performed with SS-I and SS-II only. For crystallization trials, microdrops were spotted with Oryx8 protein crystallization robot (Douglas Instruments) on 96-well plates (MRC plates, Douglas Instruments). Tiny beta subunit crystals were obtained in 3-4 days after incubating 0.5 µl of 10 mg/ml of beta subunit with an equal volume of precipitant and left to equilibrate at 20°C against the same precipitant. Two precipitants gave origin to the regular crystals we have further optimized and analyzed by X-Ray diffraction: SSII n.16 and SSII n.14. Other crystals were obtained in the following conditions: SS-I n.7 and SS-II n. 19, 20 ,30, 32, and 44. Composition of the solution used in the cited conditions are reported in Table 1.

Table 1. Precipitant conditions list.

Screening kit code	Salt	Buffer	pH	Precipitant
SS-I n.7	0.2 M ammonium acetate	0.1 M tri-sodium citrate	5.6	30 % w/v PEG 4K
SS-II n.14	0.1 M sodium chloride	0.1 M Na HEPES	7.5	1.6 M ammonium sulfate
SS-II n.16	0.05 M cadmium sulfate	0.1 M Na HEPES	7.5	1.0 M sodium acetate
SS-II n.19	None	0.1 M Na HEPES	7.5	10 % w/v PEG 8000, 8 % v/v ethylene glycol
SS-II n.20	None	0.1 M MES	6.5	1.6 M magnesium sulfate
SS-II n.30	0.5 M ammonium sulfate	0.1 M Na citrate	5.6	1.0 M lithium sulfate
SS-II n.32	None	0.1 M Na citrate	5.6	35 % v/v tert-butanol
SS-II n.44	2.0 M ammonium sulfate	None	None	5 % v/v 2-propanol

Data collection, structure determination and refinement

X-Ray diffraction data were collected at the ESRF beamline BM14U (Grenoble, France) at 100°K, without cryoprotectant. Crystals obtained with SS-II n.16

diffracted to a maximum resolution of 1.76 Å and belong to the $P2_1$ space group, with cell parameters corresponding to **a**=52.57 Å, **b**=36.48 Å, **c**=65.56 Å, and **β**=110.09°. A V_M value of 2.21 $Å^3$ Da^{-1} is compatible with the presence of 2 monomers per asymmetric unit, corresponding to a solvent content of about 44% of the cell volume. Crystals obtained with SS-II n.14 diffracted to a maximum resolution of 2.15 Å and belong to $C222_1$ space group, with cell parameters corresponding to **a**= 37.89 Å, **b**= 76.86 Å, and **c**=104.91 Å. A V_M value of 2.85 $Å^3$ Da^{-1} is compatible with the presence of 1 monomer per asymmetric unit, corresponding to a solvent content of about 57% of the cell volume.

Datasets were processed by using program MOSFLM (Leslie, 2006), merged and scaled by using SCALA (Evans, 2006), included in the CCP4 Program Suite (Collaborative Computational Project, Number 4, 1994). Statistics on data quality are reported in Table 2 and in Table 3. The structures were solved by molecular replacement, using the program Phaser (McCoy *et al.*, 2005) starting from a model built by swiss model server using the structure of notexin as template (pdb: 1AE7; Westerlund *et al.*, 1992). Statistics on the final models are reported in Tables 2 and 3. The models were initially refined by restrained molecular dynamics, minimization, and refinement steps with CNS (Brunger *et al.*, 1998). In the final cycles were employed REFMAC (Murshudov *et al.*, 1999) and SHELX (Sheldrick and Schneider, 1997), alternated by several cycles of manual adjustment and rebuilding by Coot graphic interface (Emsley and Cowtan, 2004).

The final model for crystals obtained in SS-II n.16, which includes 2044 atoms, of which 211 correspond to water molecules, was refined to a crystallographic R factor of 0.21 (R_{free}=0.23). The model obtained in SS-II n.14, includes 968 atoms, of which 51 corresponds to water molecules, and it was refined to a crystallographic R factor of 0.24 (R_{free}=0.27). Statistics concerning the quality of the final models are listed respectively in Tables 2 and 3.

Table 2. Statistics on data collection and refinement of the crystal structure obtained in precipitant condition SS-II n.16. A wavelength of 0.91232 Å was used.

Data collection	
X-ray data	Beta subunit, (SSII n16)
Wavelength [Å]	0.91232
Space group	$P2_1$
Cell parameters [Å, °]	**a**=52.57 **b**=36.48, **c**=65.56, **β**=110.09°
Resolution (Å)	33.3-1.76 (1.86 - 1.76)
Unique reflections	23192 (3236)
Multiplicity	6.1 (6.0)
Completeness (%)	99.0 (95.9)
<I/σ(I)>	8.1 (2.7)
Rmerge (%)	6.6 (27.8)
Refinement	
Total number of atoms, including solvent	211
Mean B value (Å^2)	21.17
R_{cryst}	0.21
R_{free} (5% of reflections)	0.23
Ramachandran plot preferred region (aa)	214
Ramachandran plot allowed region (aa)	18
R.m.s. on bonds length [Å], angles (°)	0.0147, 1.78

[1] The Ramachandran plot was calculated using software included in Coot platform.

Table 3. Statistics on data collection and refinement of the crystal structure obtained in precipitant condition SS-II n.14. A wavelength of 0.91232 Å was used.

Data collection	
X-ray data	Beta subunit, (SSII n14)
Wavelength [Å]	0.91232
Space group	$C222_1$
Cell parameters [Å]	**a**= 37.89 **b**= 76.86, **c**= 104.91
Resolution (Å)	36.08-2.15 (2.27 - 2.15)
Unique reflections	8636 (1239)
Multiplicity	3.0 (3.3)
Completeness (%)	99.7 (100.0)
$\langle I/\sigma(I) \rangle$	6.3 (1.6)
Rmerge (%)	11.7 (44.3)
Refinement	
Total number of atoms, including solvent	968
Mean B value ($Å^2$)	25.06
R_{cryst}	0.24
R_{free} (5% of reflections)	0.27
Ramachandran plot preferred region (aa)	111
Ramachandran plot allowed region (aa)	5
R.m.s. on bonds length [Å], angles (°)	0.021, 1.61

[1] The Ramachandran plot was calculated using software included in Coot platform.

1.7 Results and discussion

Protein crystallization and structure determination

The crystal structure of taipoxin beta subunit has been solved in two conditions at a maximum resolution of 1.76 Å. In the crystal structure obtained in SS-II n.16, two subunits define the asymmetric unit, while in condition SS-II n.14, a single one is present. Hereafter, the discussion will be referred to the highest resolution data (SS-II n.16).

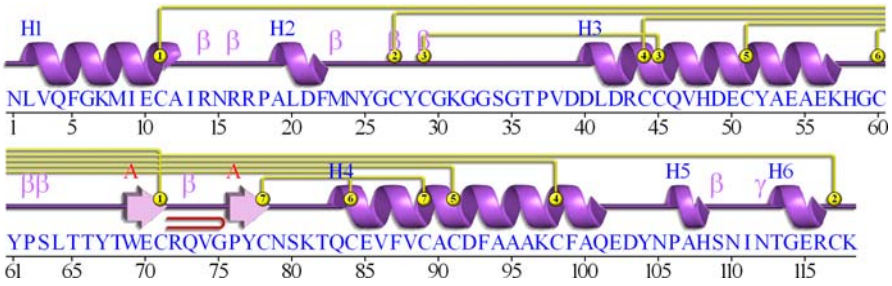

Figure 1. Topology of the subunit. Scheme draw from beta subunit PDB structure on ProFunc web site (http://www.ebi.ac.uk/thornton-srv/databases/profunc). Along the chain (purple) are shown α-helices (H) and β-sheets (A); in yellow are shown the disulfide bridge connections.

All 118 residues of beta subunit are visible and well distinguishable in the crystals. The polypeptide chain folds as expected with three α-helices, two antiparallel β-sheets and the connection loops. In particular, electron density map is well defined for the two molecules in the asymmetric unit (A and B), except for a short five-aminoacid fragment (residues Asn110 to Gly114) of chain B. The flexibility encountered in the C-terminal loop of chain B is probably due to a greater exposition to the solvent if compared to the same portion of chain A. Indeed, further analysis of the crystallographic packing, revealed that in chain A, the same fragment is involved in some interactions with a symmetrically related molecule.

As expected from structural prediction, seven disulphide bridges firmly stabilize the ternary organization. The structure starts with an α-helix (residues 1-13) partially involved in the definition of the hydrophobic channel and

connected to the β-strand via a disulfide between Cys11 and Cys71. Helix-1 and helix-3 (39-58) are separated by a fairly large loop (14-38) which contains a short α-helix and a conserved calcium binding loop (Tyr25-Gly-Cys-Tyr-Cys-Gly-Lys-Gly-Gly33). The loop is bound to the third α-helix by a conserved disulfide (Cys29-Cys45) to maintain closely spaced the three carbonyl oxygens (O28, O30, and O32) and the carboxylate of Asp49 involved in the calcium ion coordination. Two major α-helices (helix-3: 39-58; helix-4: 82-102) constitute the structural backbone of the protein and are kept tightly bound together by two S-S bridges (Cys44-Cys98; Cys51-Cys91). A major domain between helix-3 and helix-4 extends from the core of the polypeptide chain to the periphery (59-81). This region is characterized by two antiparallel β-sheets connected by a hairpin turn; notably, even this more periferic portion of the molecule, less involved in the enzymatic activity, is stabilized by two disulphide connection (Beta-1 with Helix-1 and Beta-2 with Helix-7).

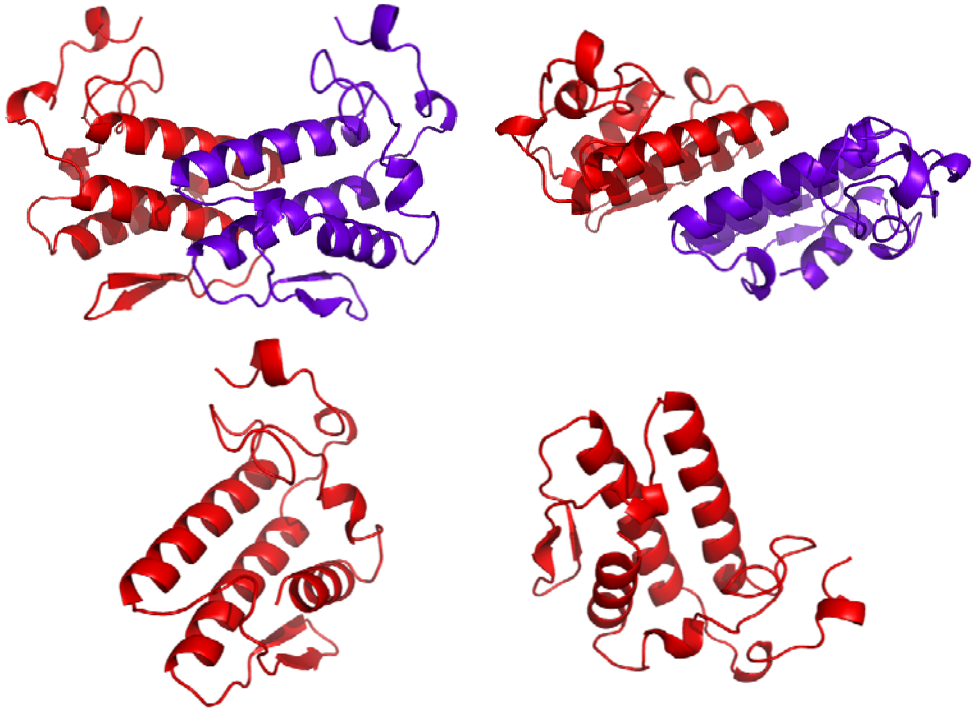

Figure 2. Multiple view of a cartoon representation of the two resolved crystal structures. Taipoxin beta subunit crystallized in a dimeric form in SS-II n.16 (top) and in the monomeric form in SS-II n.14 (bottom).

On the C-terminal end, the protein extends in a less organized twenty-aminoacids loop, whose end is kept from being too flexible and independent by a disulfide connection between Cys27 and Cys117. Topology of the subunit is shown in a schematic representation in Figure 2.

Structural considerations

Beta subunit is reported to possess very little phospholipase A_2 activity (Kini, 1997). Moreover, no neurotoxic activity of the isolated subunit on cerebellar granule neurons was observed (previous chapter). To investigate the structural basis of such low catalytic activity a comparison with available crystallographic structures of two group I PLA_2 enzymatically active neurotoxins was performed (i.e. notexin and notechis-II). An overall very conserved ternary structure was observed within the group I PLA_2. The α-helices are almost perfectly superposable, but nonetheless some structural differences are present (Figure 3).

A dissimilarity observed in the comparison with notexin, concerns the position of the loop connecting the second α-helix with the antiparallel β-strand (from Gly59 to Tyr67). A notable displacement of the considered loop occurs toward the catalytic site in the inactive beta subunit. This structural dislocation, however, appears to be present also in notechis-II structure (which is both enzymatically active and neurotoxic), suggesting little role in the orientation of this portion of the chain in the establishment of neither neurotoxic or enzymatic activity (Figure 3b).

Another difference of taipoxin beta subunit structure from the two compared neurotoxins is observed in the calcium-binding loop. The calcium-binding loop is the tract of sequence between the first two α-helices, and it is involved, with Asp49 and two water molecules in the coordination of the calcium ion. It is a conserved portion of residues 25-33 with the consensus sequence Y25-G-C-Y/F-C-G-X-G-G33. Moreover, very high flexibility is reported to be peculiar of the calcium-binding loop. According to our experimental data, the loop appears well defined in the high resolution structure, whereas there is a poor definition of the same region (suggesting elevated flexibility) in the low resolution structure. It has to be said that in both crystal structures, the Ca^{2+} could not be detected, and this could also enhance the mobility of the loop. However, the comparison with notexin and notechis-II, it reveals the calcium binding loop of taipoxin beta subunit as the most dislocated from the catalytic site. In particular, the delocalization from the active site regards the amino acids Gly30 and Gly32, involved *via* their carbonyl oxygens in the coordination of the calcium ion, and

could therefore impair the correct hydrolysis of the phospholipid substrate (Figure 3a).

Unexpectedly, no major difference in the backbone of the polypeptidic chain appears to be able to account for the lack in enzymatic activity and in neurotoxicity of taipoxin beta subunit. Moreover, the conservation of residues involved in the catalytic machinery and of the protein backbone, suggests that the cause of the lack in activity is possibly due to differences in the residues at the protein-membrane interface or involved the definition hydrophobic pocket, rather than in the malfunctioning of the hydrolytic reaction itself. In this regard, an important dislocation from the structures of both notexin and notechis-II is observed in the antiparallel β-strand, more specifically in the first of the two β-sheets and in the last portion of the loop connecting the second β-sheet with the third α-helix (Figure 3c). This antiparallel β-strand was reported to be involved in anticoagulant activity proper of PLA_2 neurotoxins and possibly in neurotoxicity (Kini and Evans, 1987; Carredano *et al.*, 1998), but further investigations need to be performed in this direction.

Observations on the surface charge distribution

Upon the consideration that the catalytic site appears very well conserved and functional, one needs to consider where else can be compromised the activity of taipoxin beta subunit. A possibility is that the protein interaction with the membranous surface is impaired by a change in the distribution of the superficial charges. As it can be noticed from the graphical elaboration in Figure 4, there is a major change in the electrostatic potential surface between the inactive beta subunit (Figure 4, left) and the active PLA_2s (Figure 4, center and right). The observed side of the protein, represents the protein/membrane interaction side, and indeed, a major change in charge distribution in the interaction surface could impair activity independently of a correct functioning of the catalytic site. However, taipoxin beta isosubunits were found to be mitogenic having neurotrophic activity on PC12 cells in culture (Lipps, 2000). This factor implies a very specific membrane binding for beta subunit. Therefore, the change in surface charge distribution may be enough to consider the possibility of different binding targets for the three subunits, but probably not sufficient to discuss about an impaired binding of beta subunit to the plasma membrane.

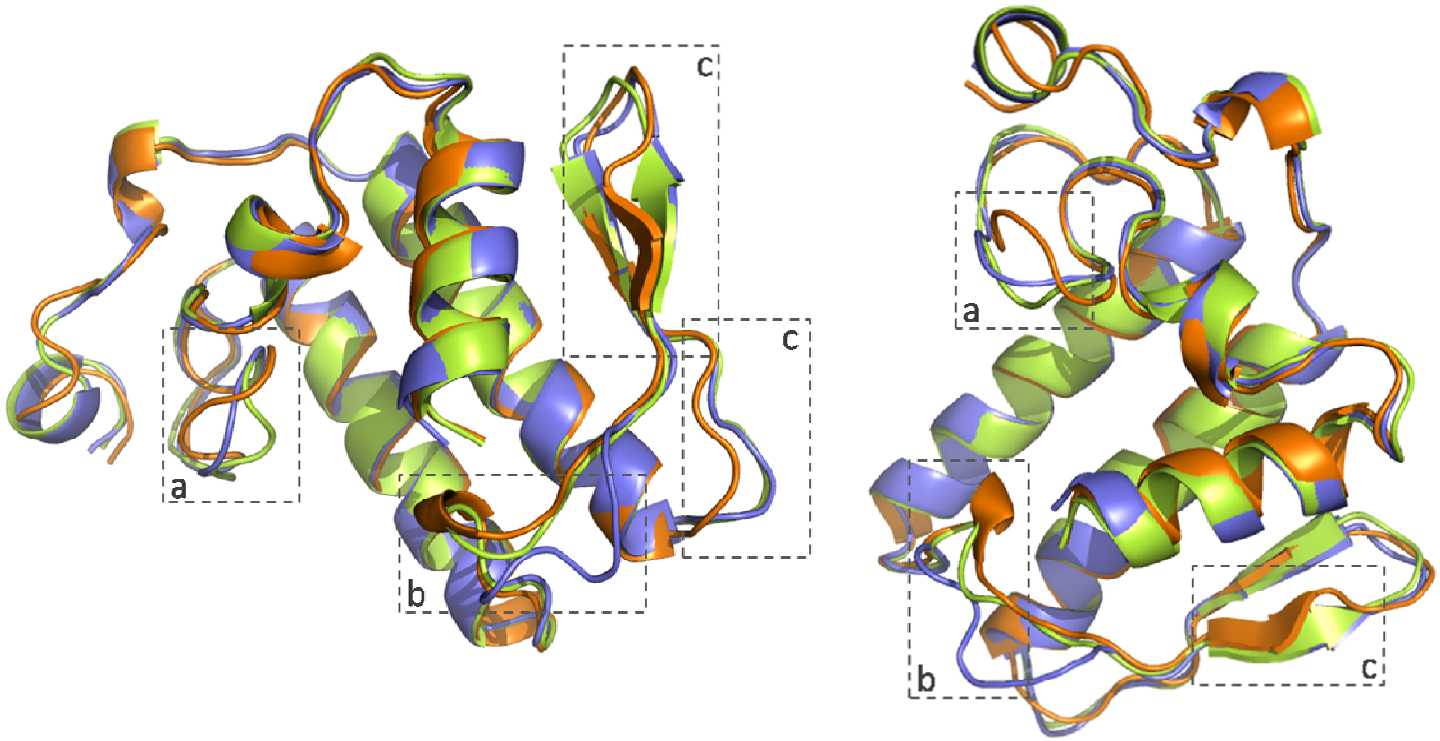

Figure 3. Structural superposition of taipoxin beta subunit (orange), notexin (blue) and notechis-II (green). Differences among the three structures are circled by the dashed line. In particular are highlighted structural differences in the calcium binding loop (a), in loop-1 (b), and in the β-strand (c).

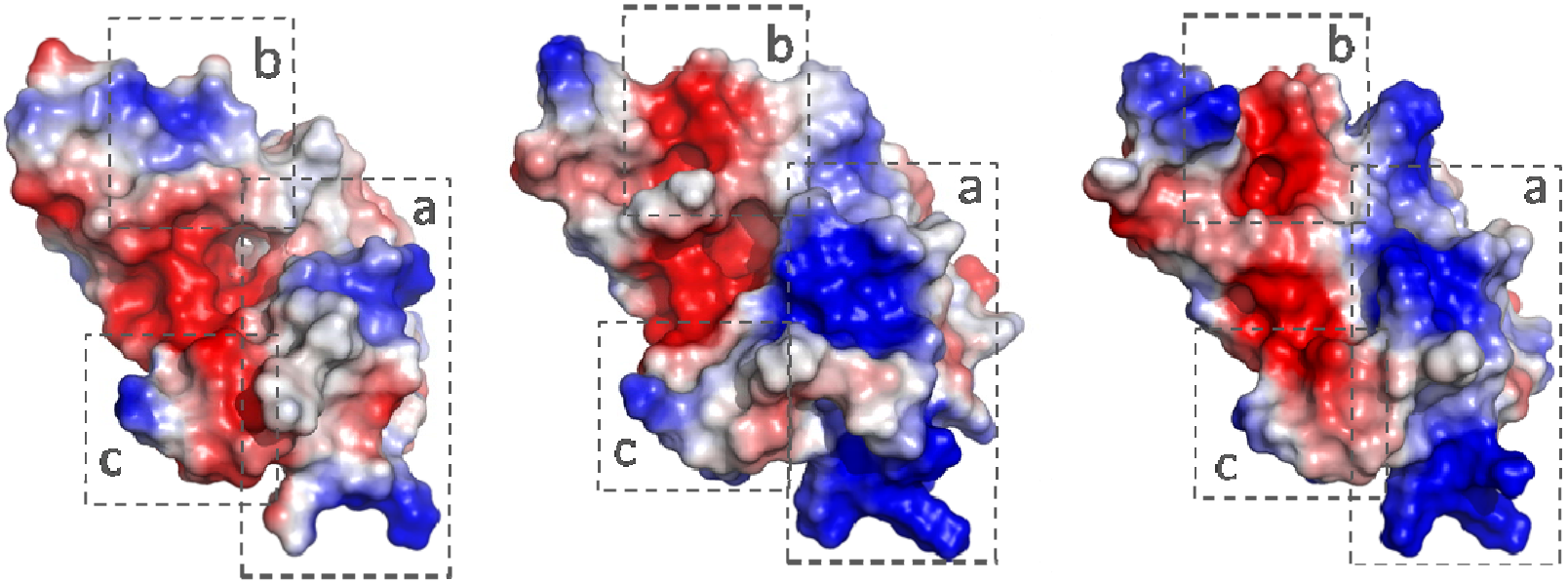

Figure 4. Electrostatic potential surface of taipoxin beta subunit (left), notexin (middle), and notechis-II (right). The orientation shows the binding pocket of the toxin with the active binding site. Positive residues are in blue, negative in red and neutral/hydrophobic residues in grey.

References

Brünger AT, Adams PD, Clore GM, DeLano WL, Gros P, et al. (1998) *Acta Crystallogr D Biol Crystallogr* 54, 905–921

Carredano E, Westerlund B, Persson B, Saarinen M, Ramaswamy S et al. (1998) The three-dimensional structures of two toxins from snake venom throw light on the anticoagulant and neurotoxic sites of phospholipase A2. *Toxicon* 36:75-92

Collaborative Computational Project, Number 4 (1994) *Acta Crystallogr D Biol Crystallogr* 50, 760–763

Evans P (2006) *Acta Crystallogr D Biol Crystallogr* 62, 72–82

Fohlman J, Eaker D, Karlsoon E, Thesleff S (1976) Taipoxin, an extremely potent presynaptic neurotoxin from the venom of the australian snake taipan (*Oxyuranus s. scutellatus*). Isolation, characterization, quaternary structure and pharmacological properties. *Eur J Biochem* 68(2):457-69

Fohlman J, Lind P, Eaker D (1977) Taipoxin, an extremely potent presynaptic snake venom neurotoxin. Elucidation of the primary structure of the acidic carbohydrate-containing taipoxin-subunit, a prophospholipase homolog. *FEBS Lett* 84(2):367-71

Fohlman J, Eaker D, Dowdall MJ, Lüllmann-Rauch R, Sjödin T, Leander S (1979) Chemical modification of taipoxin and the consequences for phospholipase activity, pathophysiology, and inhibition of high-affinity choline uptake. *Eur J Biochem* 94(2):531-40

Leslie AGW (2006) *Acta Crystallogr D Biol Crystallogr* 62, 48–57

Lind P, Eaker D (1982) Amino-acid sequence of the alpha-subunit of taipoxin, an extremely potent presynaptic neurotoxin from the Australian snake taipan (*Oxyuranus s. scutellatus*). *Eur J Biochem* 124(3):441-7

Lipps BV (2000) Isolation of subunits alpha, beta, and gamma of the complex taipoxin from the venom of Australian taipan snake (*Oxyuranus s. scutellatus*): characterization of beta taipoxin as a potent mitogen. *Toxicon* 38:1845-54

McCoy AJ, Grosse-Kunstleve RW, Storoni LC, Read RJ (2005) *Acta Crystallogr D Biol Crystallogr* 61, 458–464

Montecucco C, Gutiérrez JM, Lomonte B (2008) Cellular pathology induced by snake venom phospholipase A2 myotoxins and neurotoxins: common aspects of their mechanisms of action. *Cell Mol Life Sci* 65(18):2897-912

Murshudov GN, Vagin AA, Dodson EJ (1997) *Acta Crystallogr D Biol Crystallogr* 53:240–255

Sheldrick GM, Schneider TR (1997) *Methods Enzymol* 277:319–343

Westerlund B, Nordlund P, Uhlin U, Eaker D, Eklund H (1992) The three-dimensional structure of notexin, a presynaptic neurotoxic phospholipase A2 at 2.0 A resolution. *FEBS Lett* 301:159-164